IMPROVEMENTS IN DOA ESTIMATION BY ARRAY INTERPOLATION IN NON-UNIFORM LINEAR ARRAYS

A THESIS SUBMITTED TO
THE GRADUATE SCHOOL OF NATURAL AND APPLIED SCIENCES
OF
THE MIDDLE EAST TECHNICAL UNIVERSITY

BY

TEMEL KAYA YAŞAR

IN PARTIAL FULFILLMENT OF THE REQUIREMENTS
FOR
THE DEGREE OF MASTER OF SCIENCE
IN
ELECTRICAL AND ELECTRONICS ENGINEERING

AUGUST 2006

Approval of the Graduate School of Natural and Applied Sciences

Prof. Dr. Canan ÖZGEN
Director

I certify that this thesis satisfies all the requirements as a thesis for the degree of Master of Science.

Prof. Dr. İsmet ERKMEN
Head of Department

This is to certify that we have read this thesis and that in our opinion it is fully adequate, in scope and quality, as a thesis for the degree of Master of Science.

Assoc. Prof. Dr. Engin TUNCER
Supervisor

Examining Committee Members

Assoc. Prof. Dr. Tolga ÇİLOĞLU	(METU, EEE)	_____
Assoc. Prof. Dr. Engin TUNCER	(METU, EEE)	_____
Assoc. Prof. Dr. Aydın ALATAN	(METU, EEE)	_____
Dr. Özgür Barış AKAN	(METU, EEE)	_____
M. Sc. Ezgi GÜNAYDIN	(TÜBİTAK, SAGE)	_____

I hearby declare that all information in this document has been obtained and presented in accordance with academic rules and ethical conduct. I also declare that, as required, I have fully cited and referenced all material and results that are not original to this work.

Name Lastname : Temel Kaya YAŞAR

Signature :

ABSTRACT

IMPROVEMENTS IN DOA ESTIMATION BY ARRAY INTERPOLATION IN NON-UNIFORM LINEAR ARRAYS

YASAR, Temel Kaya
M.Sc., Department of Electrical and Electronics Engineering
Supervisor: Assoc. Prof. Dr. Engin TUNCER

August 2006, 83 pages

In this thesis a new approach is proposed for non-uniform linear arrays (NLA) which employs conventional subspace methods to improve the direction of arrival (DOA) estimation performance.

Uniform linear arrays (ULA) are composed of evenly spaced sensor elements located on a straight line. ULA's covariance matrix have a Vandermonde matrix structure, which is required by fast subspace DOA estimation algorithms.

NLA differ from ULA only by some missing sensor elements. These missing elements cause some gaps in covariance matrix and Vandermonde structure is lost. Therefore fast subspace DOA algorithms can not be applied in this case. Linear programming methods and array interpolation methods can be used to solve this problem. However linear programming is computationally expensive and array interpolation is angular sector dependent and

requires the same number of sensor in the virtual array.

In this thesis, a covariance matrix augmentation method is developed by using the array interpolation technique and initial DOA estimates. An initial DOA estimate is obtained by Toeplitz completion of the covariance matrix. This initial DOA estimates eliminates the sector dependency and reduces the least square mapping error of array interpolation. A Wiener formulation is developed which allows more sensors in the virtual array than the real array. In addition, it leads to better estimates at low SNR. The new covariance matrix is used in the root-MUSIC algorithm to obtain a better DOA estimate. Several computer simulations are done and it is shown that the proposed approach improves the DOA estimation accuracy significantly compared to the same number of sensor ULA. This approach also increases the number of sources that can be identified.

Keywords: Direction of Arrival Estimation, Nonuniform Linear Array, Array Interpolation, Root MUSIC,

ÖZ

ARTIKLI OLMAYAN DOĞRUSAL DÜZENSİZ DİZİLERDE DİZİ ARADEĞERLENDİRME İLE GELİŞ AÇISI TAHMİNİNİ GELİŞTİRME

YAŞAR, Temel Kaya
Yüksek Lisans, Elektrik ve Elektronik Mühendisliği Bölümü
Tez Yöneticisi: Doç. Dr. Engin TUNCER

Ağustos 2006, 83 sayfa

Bu çalışmada düzensiz doğrusal dizilerde (NLA), geleneksel alt-uzay algoritmalarını kullanan geliş açısı tahmini yöntemlerinin başarısını artırmak için yeni bir yöntem ileri sürülmüştür.

Düzenli doğrusal diziler (ULA) düz bir hat üzerine eşit aralıklarla yerleştirilen alıcı elemanlarından oluşur. ULA, Vandermonde matris yapısına sahip olup, bu yapı hızlı çalışan alt-uzay algoritmaları için bir gerekliliktir.

NLA'nın ULA'dan farkı sadece bazı eksik elemanlardır. Bu eksik elemanlar kovaryans matrisinde boşlukların oluşup, Vandermonde yapısının bozulmasına neden olur. Bu nedenle alt-uzay algoritmaları bu durumda kullanılamaz. Doğrusal programlama ve dizi aradeğerlendirme yöntemleri bu problemi çözebilir. Ancak doğrusal programlama işlem yükü açısından çok ağırdır. Dizi aradeğerlendirme yöntemi ise açısal bağımlılık göstermesinin yanında sanal dizi eleman sayısının gerçek eleman dizi sayısına eşit olmasını

gerektirir.

Bu tezde dizi aradeğerlendirme yöntemini ve tahmini başlangıç açılarını kullanarak, yeni bir kovaryans matrisi tamamlama yöntemi ileri sürülmüştür. Tahmini başlangıç açılarının kullanımı, açısal bölgeye bağımlılığı ortadan kaldırıp dizi aradeğerlendirmedeki en küçük kareler hatasını da azaltmaktadır. Sanal dizi eleman sayısının gerçek dizi eleman sayısından fazla olmasını sağlayan Wiener formülasyonu geliştirilmiştir. Ayrıca düşük SNR seviyelerinde daha iyi tahminler alınmasını da sağlamıştır. Elde edilen yeni kovaryans matrisi, daha iyi sonuçlar almak için kök-MUSIC algoritmasında kullanılmıştır. Çeşitli bilgisayar simülasyonları gerçekleştirilmiştir ve gösterilmiştir ki, önerilen yöntem aynı sayıda elemana sahip ULA'ya göre DOA tahmininde kaydadeğer bir gelişme sağlanmıştır. Bu yöntem ile ayrıca daha fazla sayıda kaynak tespit edilebilmektedir.

Anahtar sözcükler: Geliş Açısı Tahmini, Düzensiz Doğrusal Diziler, Dizi Aradeğerlendirmesi, Kök MUSIC

in loving memory of Ayça

ACKNOWLEDGMENTS

I would like to express my thanks to my supervisor Assoc. Prof. Dr. Engin TUNCER for his guidance and support during the preparation of this study.

I would like to thank my wife Demet for her all kind of support, understanding and being a so lovely wife.

TABLE OF CONTENTS

PLAGIARISM iii

ABSTRACT iv

ÖZ vi

ACKNOWLEDGEMENTS ix

TABLE OF CONTENTS x

CHAPTER

1 INTRODUCTION 1
- 1.1 Applications of DOA Estimation with Sensor Arrays 1
- 1.2 Sensor Arrays and Sources 5
- 1.3 Focus of The Thesis 8

2 DOA ESTIMATION WITH ULA 10
- 2.1 System Model 10
  - 2.1.1 Assumptions 10
  - 2.1.2 Uniform Linear Arrays 12
  - 2.1.3 Signal-Model 14
- 2.2 Algorithms 19
  - 2.2.1 Non-Parametric Algorithms 20

2.2.2 Parametric Subspace Algorithms 23
2.2.3 Cramer-Rao Lower Bound 29

3 DOA ESTIMATION WITH NLA 31
3.1 Co-Array 31
3.2 Array Types 32
3.2.1 Optimum Arrays 34
3.2.2 Sub-Optimum Arrays 34
3.3 Covariance Matrix Augmentation Methods 37
3.3.1 Fully Augmentable Arrays 38
3.3.2 Partially Augmentable Arrays 39

4 PROPOSED METHOD 42
4.1 Introduction 42
4.2 Problem Formulation 44
4.3 Array Interpolation 45
4.4 Covariance Matrix Augmentation and DOA Estimation 46

5 PERFORMANCE EVALUATION OF THE PROPOSED METHOD 48
5.1 Conventional Number of Sources 49
5.1.1 One Source 49
5.1.2 Two Sources 49
5.1.3 Three Sources 57
5.1.4 Four Sources 62
5.1.5 Five Sources 67
5.2 Superior Case 70

5.2.1 Six Sources 70
5.2.2 Seven Sources 70

6 CONCLUSION 73
6.1 Advantages 73
6.1.1 Number of Sources 74
6.1.2 Resolution 74
6.1.3 Independency of Angular Sector 74
6.1.4 Low Computational Complexity 75
6.2 Disadvantages 75
6.2.1 Ambiguities 76
6.2.2 Multi-Path 76

REFERENCES 76

LIST OF TABLES

3.1 Recurrence of Lags 32
3.2 Summary of Leech's Suboptimal Min-Redundant Sequences . . 36
3.3 Summary of Sverdlik's Suboptimal Non-Redundant Sequences 37

LIST OF FIGURES

1.1 Airborne RADAR Example 2
1.2 Active SONAR Example 3
1.3 Seismology Example 4
1.4 Uniform Linear Array in x-axis 6

2.1 Cardioid Amplitude Response 13
2.2 Planar Wave Impinging on ULA 18
2.3 Tapped Delay Line Structure Spatial Filter 21
2.4 Roots of (2.73) 25
2.5 Sensors Positioned Suitable for ESPRIT Algorithm 27

3.1 NLA with Corresponding Inter-Element Distances 33
3.2 Co-Array Scheme 33
3.3 Co-Array Scheme ULA 34
3.4 Co-Array Scheme Optimum NLA 34
3.5 Co-Array on top is a restricted minimum redundant array, co-array at bottom is an unrestricted minimum redundant array. 35
3.6 Co-Array on top is a non-redundant array with consecutive gaps, co-array at bottom is a non-redundant array with separate gaps. 38

5.1 Performance for one source located at 60 degrees with increasing SNR. 50
5.2 Performance for one source which is moving from 10 to 170 degrees. 51
5.3 Performance when the source at 90 degrees is fixed and a second source is swept. 52

5.4 Performance of the algorithms for increasing SNR when two sources are located at 55 and 60 degrees respectively. 53
5.5 Performance of the algorithms for the number of snapshots when two sources are located at 55 and 60 degrees. 54
5.6 Performance for two sources located at 60 and 140 degrees with respect to increasing SNR. 55
5.7 Performance for two sources located at 60 and 140 degrees with respect to increasing number of snapshots. 56
5.8 Condition Number of Inverse Term in (4.5) for two sources located at 60 and 50 degrees with respect to increasing SNR. . 58
5.9 Condition Number of Inverse Term in (4.5) for one source located at 90 other source swept 30 to 89 degrees. 59
5.10 Performance of Wiener formulation for two sources located at 50 and 60 degrees with respect to increasing SNR. 60
5.11 Performance of Wiener formulation for one source located at 90 other source swept 30 to 89 degrees. 61
5.12 Performance for three sources located at 56, 60 and 64 degrees with respect to increasing SNR. 62
5.13 Performance for three sources located at 56, 60 and 64 degrees with respect to increasing number of snapshots. 63
5.14 Performance for two sources located at 56 and 60 degrees, third one is moving 10 to 170 degrees. 64
5.15 Performance of three sources fixed at 55, 61 and 67 degrees and the fourth source is swept 30 to 150 degrees. 65
5.16 Performance for four sources located at 55, 60, 65 and 120 degrees respectively. 66
5.17 Performance for five sources located at 50, 60, 70, 80 and 90 degrees with respect to increasing SNR. 67

5.18 Performance for five sources located at 50, 60, 70, 80 and 90 degrees with respect to increasing number of snapshots. 68
5.19 Performance for four sources located at 50, 60, 70 and 80 degrees, fifth one is moving 10 to 170 degrees. 69
5.20 Performance for six sources located at 60, 70, 80, 90, 100 and 110 degrees with respect to increasing number of snapshots. . 71
5.21 Performance for six sources located at 30, 50, 70, 90, 110 and 130 degrees, seventh one is moving 10 to 170 degrees. 72

CHAPTER 1

INTRODUCTION

1.1 Applications of DOA Estimation with Sensor Arrays

For a century, importance of finding the arrival angle of a target by using sensor arrays is preserved as shown in some early studies [1], [2]. A target can be located only by receiving some kind of signal, or one may call it energy, from it. This energy may be electromagnetic energy, acoustic wave, seismic waves, etc. This signal can be radiated directly from target itself (active target) or this signal may be reflected from target (passive target), where the signal is emitted from some other known source. Active targets that radiate energy may be a speaking human being, an earthquake, a cellular phone, etc. A passive target may be a submarine that reflects the SONAR pulses, or an aircraft that reflects the RADAR pulse of surveillance RADAR. This signal is acquired via sensor arrays. These sensors convert the energy, which is emitted or reflected by target, into the electrical signals. Hence, there are many sensor types depending on the application, the energy type, frequency band, etc.

Many applications, such as RADAR, SONAR, seismology, astronomy, medical sciences, communications, music, speech processing, etc are successfully running with the help of these studies that have been conducted and still being conducted as in this thesis. A few direction of arrival estimation applications are introduced in following paragraphs to express how broad the

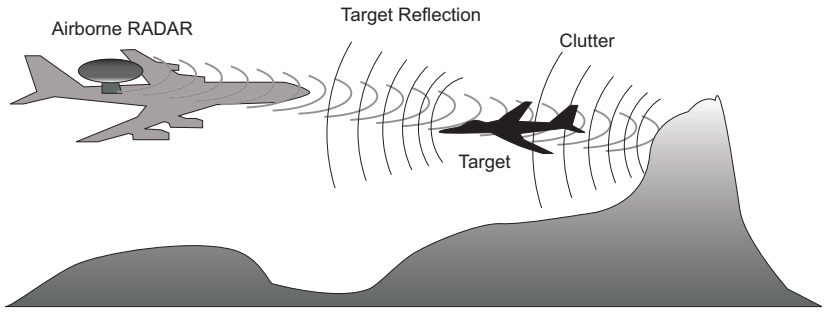

Figure 1.1: Airborne RADAR Example

topic is.

In RADAR applications, electromagnetic signals both transmitted and received via antenna arrays. RADAR can be airborne, ground or shipped based but all of them have same principle. Jamming, which appears in military application almost all the time, the multipath and clutter phenomena (Figure 1.1), are the problems that arise in front of the engineers. For further references one may examine [3].

In radio astronomy usually very large size radio antennas are being used in large scale antenna arrays, i.e. up to thousands of kilometers for inter antenna distances [4]. Those structures confront the atmospheric obstacles such as different kind of layers that cause diffraction, distortion and reflection. Also movement of earth results in movement of array elements which is another kind of difficulty.

For speech applications one of the hot topics is to locate a speaker in room of size small one to a large conference hall, and extract the speakers sound from all other sound sources and noise in that room by using microphone arrays located on the walls of that room [5]. Therefore cumbersome process of passing a microphone from speaker to speaker or ambient noise in background is of no problem anymore.

SONAR applications can be divided into two main branches. First one

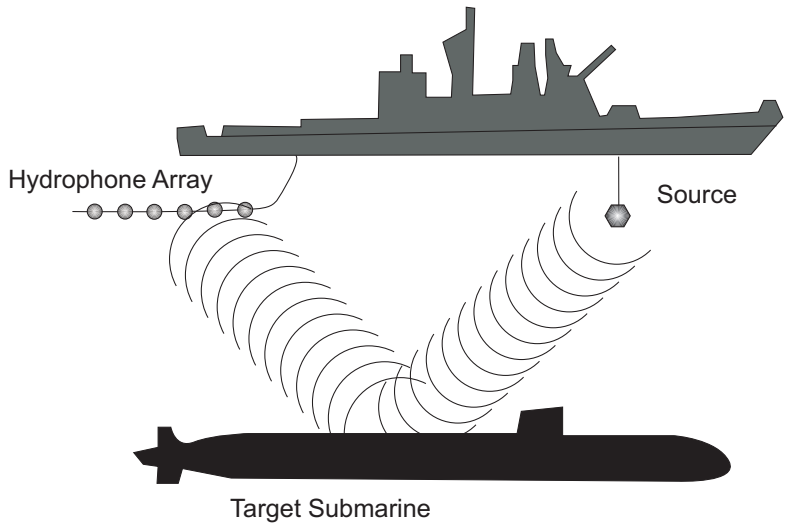

Figure 1.2: Active SONAR Example

is active SONAR. This type of SONAR works by sending a known acoustic pulse under water and listen the reflection by a hydrophone array as in Figure 1.2. Second one is passive SONAR. Passive SONAR just listens the environment again by hydrophone arrays as in active SONAR. Both type have some difficulties because underwater environment is different and harsher than air [6].

Seismology deals mostly with constructing the underground image of earth. An explosion of under control radiates wave along different layers of earth and reflections are recorded via geophone arrays as illustrated in Figure 1.3. Usually a specific layer is of interest such as oil reserve, coal reserve, special layers that posses fossils etc [7]. This usage has similar idea as in active SONAR applications. Also detecting the exact location and power of earthquakes is another usage of geophone arrays. But this system is a passive one as in passive SONAR systems.

In communication systems, in order to avoid multipath effect and enemy jamming array antennas are useful due to beamforming capability. Especially

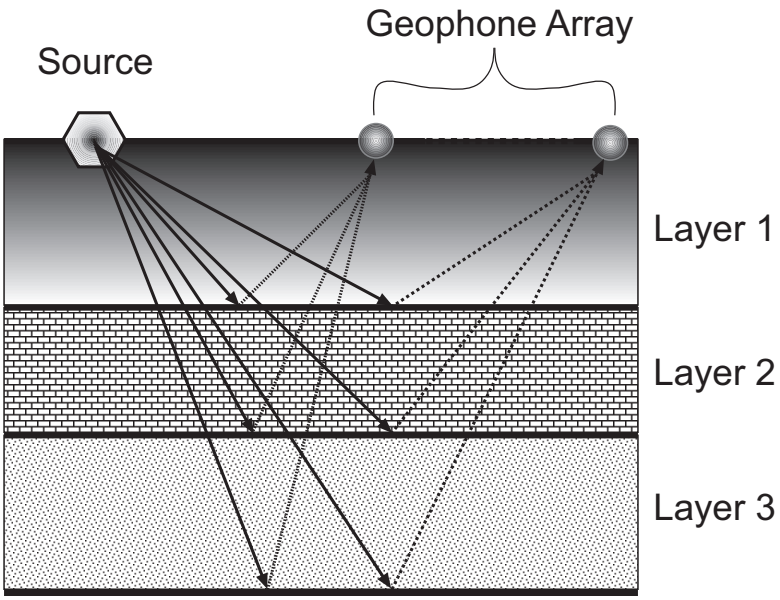

Figure 1.3: Seismology Example

in satellite communication systems both in ground side and satellite side have arrays to increase the communication performance and security via enhanced directivity. Also in wireless cellular communication systems array antennas improve the system performance significantly [8], [9].

Sensor arrays are widely used in medical imaging especially for ultrasound applications. Due to complicated structure of human body, observing the layers of body inherently possesses incredible amount of difficulties. Therefore sensor arrays with large number of elements are used in this discipline [10] to resolve ultrasonic reflections from different layers of the body.

As a result sensor arrays have many important applications in almost every discipline of electrical engineering. It would be worth to increase efficiency and decrease the cost of arrays because some sensors like radar antennas, radio astronomy antennas can cost millions of YTL. Increasing the performance by more advanced hardware is an option but an expensive option. Software

improvements are so successful that, it is nearly not possible to advance furthermore. So the only option left is to decrease the hardware cost while keeping the software performance steady as much as possible. Therefore aim of this thesis is when the unnecessary array elements are removed how to process available data left effectively in order to keep the degradation of the performance as low as possible.

In this thesis working with sound that human can hear is chosen because equipment to be used such as microphones, analog to digital converters (ADC), digital signal processor (DSP) board is much more convenient than any other type of equipment. DSP boards and ADC cards are much cheaper due to low frequency band. Also working with hydrophones, geophones or antennas would not be practical due to higher mismatch probability of sensor elements from each other. Additionally it would be easier to predict the flaws of experiment environment for acoustic waves than electromagnetic or seismic waves. But method proposed in this thesis is applicable to any kind of sensor array because they all based on same mathematical structure.

1.2 Sensor Arrays and Sources

Before detailed information is presented, it would be better to introduce the type of arrays and sources that is considered in this thesis.

The sensor array in our discussion is linear sensor array positioned in x-axis as illustrated in Figure 1.4. Sensors are spaced equally with distance d in uniform linear arrays and they are spaced integer multiples of d in non-uniform linear arrays. All sensors are assumed to be calibrated, in other words they have same amplitude and phase characteristics. Sensors amplitude response does not depend on incoming signals direction, i.e. they are all omni directional. There assumed to be no reflective object in the environment, i.e. there is no multi-path phenomena as in Figure 1.1 also sensors

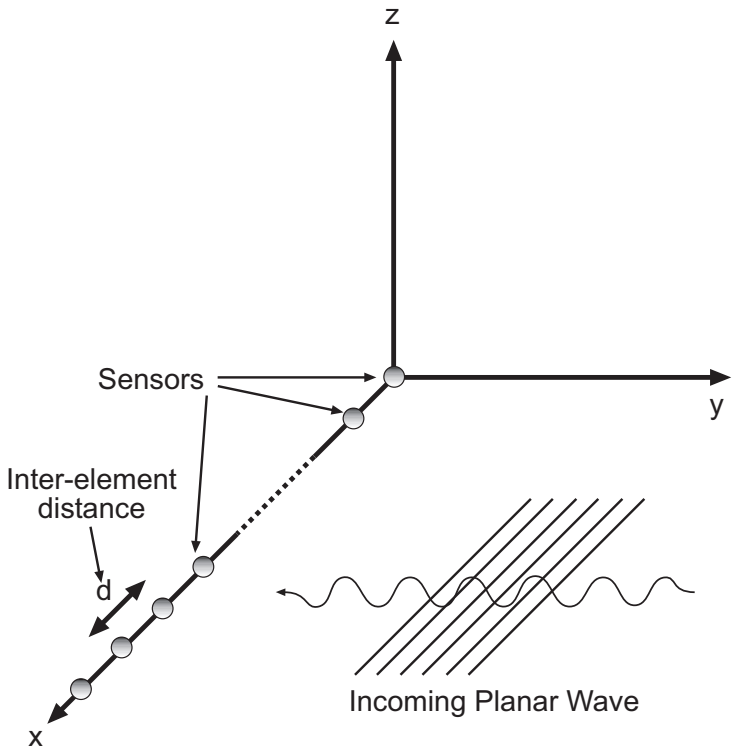

Figure 1.4: Uniform Linear Array in x-axis

do not affect each other in any sense. Whole system is linear time invariant (LTI), therefore superposition principle can be applicable for incoming signals coming from different sources.

For an acoustic source, general equation of a sound wave in three dimensional space is defined as,

$$\nabla^2 p(\xi, t) = \frac{1}{c^2} \frac{\partial^2 p(\xi, t)}{\partial t^2} \text{ [11]} \tag{1.1}$$

where c is the speed of sound, ξ is the (three-dimensional) space coordinate system, t is time and $p(\xi, t)$ is the pressure of sound wave at location ξ and time t. In our discussion, sound sources are assumed to be far enough that sound waves reach the sensor array as plane waves. This plane wave is impinging on x-z plane as in Figure 1.4. The solution of the equation for

planar real sound wave is

$$p(\xi, t) = Pe^{-j(\omega/c)\xi t} + Pe^{-j(-\omega/c)\xi t} \tag{1.2}$$

Where $\omega = 2\pi f$ is the carrier frequency of the signal in radians per second and P is the amplitude of incoming signal. Note that there is an implicit assumption of incoming signal is a narrowband modulated signal around the frequency ω. This point is mathematically clarified later in section 2.1.1. In this chapter it is sufficient to assume incoming signal is just a complex exponential at a fixed frequency ω. Negative frequency component of $p(\xi, t)$ is filtered out because it behaves as a virtual source located at negative angle of positive frequency component.

Data observed (call as $y_0(t)$) from reference sensor, which may be located at leftmost, rightmost or any other position in array, can be formulated as follows assuming the negative frequency is filtered out.

$$y_0(t) = P_0 e^{-jwt/c} \tag{1.3}$$

Data observed from other sensors is just the time delayed version of reference sensors. This time delay depends not on the coordinates of source but merely on the source angle (θ) with respect to normal of linear array because of far field assumption that results in planar waves. Hence,

$$y_k(t) = P_k e^{-j2\pi f(t-\tau_k(\theta))/c} \tag{1.4}$$

where $\tau_k(\theta)$ is the time delay with respect of incoming signal directed from angle θ from reference sensor to k^{th} sensor.

In the following section focus of the thesis is defined based on the array and sources described in this section.

1.3 Focus of The Thesis

To focus on the subject and simplify the mathematical interpretations, uniform linear arrays (ULA) are chosen to be starting point for developing new ideas in this thesis. Uniform linear arrays are defined as sensor elements positioned on a straight line with equal inter element distances, as illustrated in Figure 1.4. This structure has a special mathematical advantage that allows algorithms to be composed of simple matrix operations. In addition to that, unknown parameter of the problem reduces to single dimension, which is azimuth of arrival angle. Once the idea is solidified over linear arrays, it would be probable to extend the idea into non-linear arrays, i.e. two or three dimensional arrays.

There are some algorithms that require ULA sensor structure, such as root-MUSIC [12], MUSIC [13], Capon [14]. In addition to those there are some other algorithms that can work with NLA, while ULA structure is also acceptable such as ESPRIT [15]. Note that Capon's algorithm is just given for reference because it is not a subspace algorithm that this thesis is based on. Performance analysis of these algorithms with ULA were deeply investigated by researchers [16], [17], [18], [12]. These well known sub-space algorithms are so improved for different cases that they nearly stick to the related Cramer-Rao bound (CRB) [19].

Therefore researchers took another path to further improve the performances of subspace algorithms with linear sensor arrays. When some loose conditions are assumed [20], distributing the array sensors non-uniformly according to some criteria, redundant information of uniformly spaced linear arrays return as new information and higher performance results. The non-uniform linear array (NLA) term is defined in this context as a ULA with some missing elements as illustrated in Figure 3.1. There are two major achievements of NLA, when it is interpolated to same aperture size ULA.

First, since distance between the sensors at two end points is increased compared to ULA that has the same number of elements, capability of resolving two closely spaced targets is increased. Second, number of targets that can be estimated by subspace algorithms such MUSIC or ESPRIT is higher than the ULA case because increase in the aperture size reveals more covariance lags between sensor elements than in ULA, which has the same number of elements. More covariance lags increases the dimension of space represented by the data obtained from inter-element distances. Since number of sources that can be detected by subspace algorithms is limited by space dimension spanned by array, NLA can detect more sources than ULA for the same number of sensor elements.

There are also some drawbacks of this approach. In most of the NLAs there are some missing information due to wrong placement of sensor elements or intentionally arranged large aperture size for some other reasons that is discussed in upcoming chapters. So the space that should be spanned by array can not be obtained directly due to missing information. If those missing information somehow can not be estimated successfully, DOA algorithms diverge from the correct solution.

Therefore the problem here can be defined as filling the missing information in NLA structures defined above such that NLA can be usable by subspace algorithms that strictly requires ULA structure. There are some approaches in literature to fulfil the missing values [21], [20], [22] that require some burden to user such as linear programming, limitation on distribution of sources in space. This study proposes an alternative solution for estimation those missing values with less computational complexity and less restrictions on the location of sources. In addition to bringing out a solution to the problem defined above using a NLA instead of ULA provides better performance for subspace algorithms, when number of elements in NLA and ULA are same.

CHAPTER 2

DOA ESTIMATION WITH ULA

2.1 System Model

system is described mathematically in this section before mentioning any kind of DOA estimation algorithms. This mathematical model is valid throughout the discussion and all algorithms are based on same model and notations.

2.1.1 Assumptions

Prior to constructing the system there are few important assumptions to be made for the model. The first one is, sources are assumed to be far enough to sensor array so that waves impinging on the array are planar waves. The second one is, system is assumed to be linear time invariant. Third, sources are uncorrelated with each other. Last one is, noise in the sensor is spatially and temporally uncorrelated.

Far Field Assumption

Since it is assumed that sources are far enough to sensors, waves impinging upon sensors are planar [23]. Planar waves create just constant phase difference between consecutive sensor elements that is denoted as τ in this chapter.

If far field assumption does not hold, i.e. sources are in near field, all sensors have some additional phase depending on the location of the source. For this case, coordinate of sources must be taken into account so that the search extends to two dimensions and it is not be easy to model the system. If location of the source, which is in near field, is ignored and calculations are done according to far field assumption, unknown phase degrades the performances of algorithms severely. Fortunately, except for speech applications that take place in a small room, far-field assumption holds.

Therefore it is reasonable to assume that sources are in far field in this thesis.

Linear Time Invariance

All parts of the system are assumed to be linear time invariant (LTI). The system this composed of sources, medium (air, water, solid objects such as earth, flesh, etc) that a wave travels through, sensor elements (microphones, hydrophones, geophones, transducers, antennas, etc), cables, contact points and electronic equipment such as (amplifiers, mixers, demodulators, analog to digital converters, digital signal processing boards, etc).

LTI assumption significantly reduces the complexity of calculations as in all other applications of signal processing. Especially for subspace algorithms, most of the time covariance information of incoming data is the heart of algorithms, so instead of working with time values just lag values of inter-elements provide simple matrix computations.

Another important benefit of LTI assumption in DOA estimation is to use superposition principle for multiple sources. Therefore solving the DOA problem for one source is no different than multiple sources for subspace algorithms as long as sources are uncorrelated. Correlation of sources is another point in DOA estimation that is pointed out in the following subsection.

Correlation of Sources

The presence of coherent sources is an important problem for subspace DOA estimation algorithms. Coherent sources emerge usually via multipath effect, clutter and enemy jamming process. These effects appear almost all the time in real life applications. Several spatial smoothing methods [24], [25], [26] are developed in order to overcome coherent sources problem.

Along this thesis correlation issue is not the primary concern therefore all sources are assumed to be uncorrelated unless otherwise stated. In addition to that, multipath effect and jamming are out of the scope for this discussion.

Noise

Data observed in sensor elements consists of signals and noise components. In general signal component includes both the source of interest and other unwanted sources such as jammer or reflections. So, noise is primarily the ambient environment noise and thermal noise in all electronic equipment. The noise is assumed to be temporally and spatially stationary, zero-mean white Gaussian and statistically independent of the signals term. It is also assumed that there is no correlation between the noises of the different sensors, i.e.,

$$E\{e_k(t)e_i(t)\} = \delta_{k,i}(t) \tag{2.1}$$

where $e_k(t)$ is the noise of k^{th} sensor at time t.

2.1.2 Uniform Linear Arrays

Uniform linear arrays are defined as sensor elements located on a straight line with equal inter-element distances d as illustrated in Figure 1.4. The value of d may vary from the frequency band that is under consideration to resolution required or to precession required. This value is clarified mathematically in section 2.2.

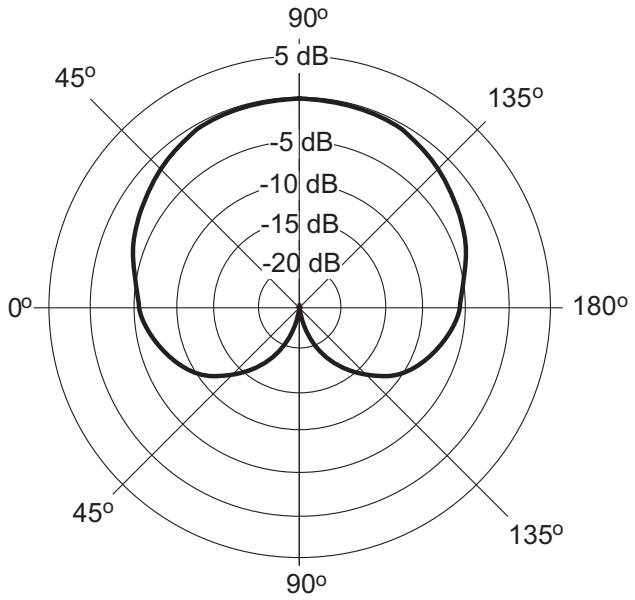

Figure 2.1: Cardioid Amplitude Response

Sensors are assumed to be omni directional although in practice this is not the case. For DOA estimation algorithms using uniform linear arrays, a source, which is in front of the array, and another source, which is behind the array and at the same angle, creates same data in the sensors. This property of linear arrays creates a confliction. So ULA is used for finding sources that are located in front of the array. It is assumed that there is no source behind the array. This condition removes the necessity of sensors to be omnidirectional but they should have a cardioid shape (Figure 2.1) of amplitude response that can be approximated as half omni-directional. It is worth recall 2.1.1 that all sensors are linear time invariant.

There are some practical problems about positioning the sensor elements in their exact location. Actually it is nearly impossible to implement them precisely due to errors of the machines used in construction. This error appears as an unknown phase component in calculations. There are some

methods [27], [28] to overcome these issues but throughout this discussion all the sensors are assumed to be located at exact positions.

2.1.3 Signal-Model

In order not to introduce new notations and create confliction with DOA estimation literature, system model developed by Stoica in [29] is summarized in this chapter according to purposes of the discussion.

Let $x(t)$ is the signal recorded at some reference point. This reference point can be a sensor in the array or some other location outside the array but not too far from array that far field assumption with respect to source still holds.

Until signals are digitized for processing, all signals are continuous real signals so variable t is a continuous variable.

Time required for planar wave to travel from reference point to k^{th} sensor is denoted by τ_k where $k = 1, \ldots, m$ (sensor number in array). Let all sensors have known individual impulse response as $\bar{h}_k(t)$. And let there is some noise in each sensor called $\bar{e}_k(t)$ that may be thermal noise originated or ambient noise, as defined in section 2.1.1. Therefore signal in k^{th} sensor can be written as,

$$\bar{y}_k(t) = \bar{h}_k(t) * x(t - \tau_k) + \bar{e}_k(t) \tag{2.2}$$

where $*$ is the convolution operator. Here $x(t)$ and τ_k are unknown. By estimating time delay value of τ_k arrival angle of the source can be estimated assuming $\bar{h}_k(t)$ and geometry of sensor array are all known.

Up to this point model obtained in (2.2) is not be useful for most of the algorithms. In order to construct a more useful model, incoming signals should be narrow band. It is easier to construct this model in frequency domain. Let $\bar{Y}_k(\omega), \bar{H}_k(\omega), \bar{E}_k(\omega)$ and $X(\omega)$ are the fourier transforms of $\bar{y}_k(t), \bar{h}_k(t), \bar{e}_k(t)$ and $x(t)$ respectively. (2.2) can be rewritten in frequency

domain as,

$$\bar{Y}_k(\omega) = \bar{H}_k(\omega)X(\omega)e^{-j\omega\tau_k} + \bar{E}_k(\omega) \tag{2.3}$$

Except for speech applications, energy spectral density of $x(t)$ has a bandpass characteristics with the center frequency ω_c, which may be called carrier frequency. $x(t)$ is obtained from modulation of the baseband signal $s(t)$ whose fourier transform is denoted by $S(\omega)$.

Before further advancing, there are few points to be cleared out about modulation process. Although there is no complex modulated signal in real life, it is important to introduce it for digital processing of modulated signal in a computer. If $s(t)$ is multiplied by $e^{j\omega_c t}$, $S(\omega)$ shifts to the right in frequency spectrum while $\omega_c > 0$.

$$S(\omega) = \int_{-\infty}^{+\infty} s(t)e^{-j\omega t}dt \tag{2.4}$$

$$\Rightarrow \int_{-\infty}^{+\infty} s(t)e^{j\omega_c t}e^{-j\omega t}dt = \int_{-\infty}^{+\infty} s(t)e^{-j(\omega-\omega_c)t}dt = S(\omega-\omega_c) \tag{2.5}$$

After complex modulation, signal becomes complex valued because symmetricity of power spectrum is vanished. Since modulated signal in real life has even spectrum $X(\omega)$ should be in form as,

$$X(\omega) = S(\omega-\omega_c) + S^*(-(\omega+\omega_c)) \tag{2.6}$$

Demodulation process can be done via multiplying $x(t)$ with $e^{-j\omega_c t}$. That results in $S(\omega) + S^*(-\omega-2\omega)$ which is shifted version of $X(\omega)$ to left in frequency domain. This signal has two components, which are baseband $S(\omega)$ and bandpass component $S^*(-\omega-2\omega)$. As putting these information into the (2.3), following form of sensor output is obtained in terms of modulated signal in frequency domain,

$$\bar{Y}_k(\omega) = \bar{H}_k(\omega)[S(\omega-\omega_c) + S^*(-\omega+\omega_c)]e^{-j\omega\tau_k} + \bar{E}_k(\omega) \tag{2.7}$$

demodulate $\bar{y}_k$ and obtain $\tilde{y}_k$ as,

$$\tilde{y}_k(t) = \bar{y}_k(t)e^{-j\omega_c t} \tag{2.8}$$

In frequency domain,

$$\tilde{Y}_k(\omega) = \bar{H}_k(\omega+\omega_c)[S(\omega) + S^*(-\omega-2\omega_c)]e^{-j(\omega+\omega_c)\tau_k} + \bar{E}_k(\omega+\omega_c) \tag{2.9}$$

Pass $\tilde{Y}_k(\omega)$ through a low-pass filter to eliminate higher frequency term $S^*(-\omega-2\omega_c)$ term and obtain,

$$Y_k(\omega) = H_k(\omega+\omega_c)S(\omega)e^{-j(\omega+\omega_c)\tau_k} + E_k(\omega+\omega_c) \tag{2.10}$$

where $H_k(\omega+\omega_c)$ and $E_k(\omega+\omega_c)$ are low-pass components of $\bar{H}_k(\omega+\omega_c)$ and $\bar{E}_k(\omega+\omega_c)$ respectively.

Now narrowband assumptions takes its place as, $|S(\omega)|$ decreases rapidly with increasing $|\omega|$. To make this assumption valid following conditions should be met [30],

$$BW \times \Delta\mathrm{T}_{max} \ll 1 \tag{2.11}$$

BW is the bandwidth of $s(t)$ and $\Delta\mathrm{T}_{max}$ is defined as,

$$\Delta\mathrm{T}_{max} \triangleq \max_{n,m=0,\ldots,N-1}\{\Delta\mathrm{T}_{nm}\} \tag{2.12}$$

where $\Delta\mathrm{T}_{nm}$ is the travel time of incoming signal between n^{th} and m^{th} sensors. Hence (2.10) can be realized as,

$$Y_k(\omega) = H_k(\omega_c)S(\omega)e^{-j\omega_c\tau_k} + E_k(\omega+\omega_c) \tag{2.13}$$

There is an implicit assumption of sensor array frequency response is flat around ω_c i.e. $H_k(\omega+\omega_c) = H_k(\omega_c)$. When the inverse fourier transform of (2.13) taken,

$$y_k(t) = H_k(\omega_c)e^{-j\omega_c\tau_k}s(t) + e_k(t) \tag{2.14}$$

can be obtained while $e_k(t)$ is assumed to be inverse fourier transform of $E_k(\omega+\omega_c)$ which does not effect the calculations of DOA algorithms following in this chapter.

In order to obtain y vector that contains recorded data of sensor elements, steering vector $\mathbf{a}$ is defined as follows,

$$\mathbf{a}(\theta) = [H_1(\omega_c)\ e^{-iw_c\tau_1}...H_m(\omega_c)e^{-iw_c\tau_m}]^{\mathrm{T}} \tag{2.15}$$

Transfer functions of sensors and geometry of array is known. So $\tau_1, ..., \tau_m$ contain the information of arrival angle and they are functions of θ. That explains why is $\mathbf{a}$ is function of θ. This is clarified later. Note that since all sensors are assumed to be omni-directional as defined in section 2.1.1, $H_k(\omega)$ are independent of θ. Now 2.14 can be written in vector form as,

$$\mathbf{y}(\theta) = \mathbf{a}(\theta)s(t) + \mathbf{e}(t) \tag{2.16}$$

where

$$\mathbf{y}(\theta) = [y_1(t)...y_m(t)]^T \tag{2.17}$$

$$\mathbf{e}(\theta) = [e_1(t)...e_m(t)]^T \tag{2.18}$$

When all sensors are assumed to be identical and first sensor is taken to be the reference point, steering vector can be transformed to following equation,

$$\mathbf{a}(\theta) = [1\ e^{-iw_c\tau_1}...e^{-iw_c\tau_{m-1}}] \tag{2.19}$$

For multiple sources define the steering matrix $\mathbf{A}$

$$\mathbf{A} = [\mathbf{a}(\theta_1), \ldots, \mathbf{a}(\theta_n)] \tag{2.20}$$

Since it is assumed that the system is an LTI system, superposition principle can be used as,

$$\mathbf{y}(t) = [\mathbf{a}(\theta_1), \ldots, \mathbf{a}(\theta_n)] \begin{bmatrix} s_1(t) \\ \vdots \\ s_n(t) \end{bmatrix} + \mathbf{e}(t) \triangleq \mathbf{A}\mathbf{s}(t) + \mathbf{e}(t) \tag{2.21}$$

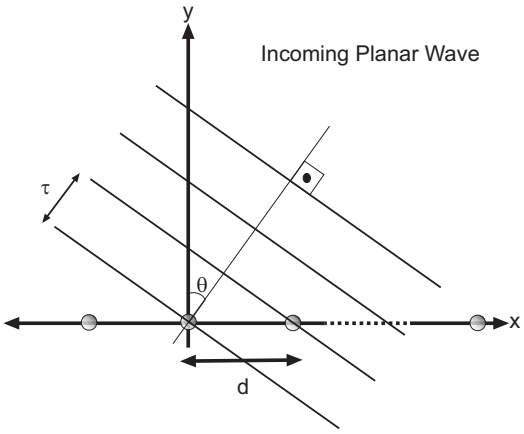

Figure 2.2: Planar Wave Impinging on ULA

where

$$\theta_k = \text{DOA angle of } k^{th} \text{ source} \tag{2.22}$$

$$s_k(t) = \text{Signal of } k^{th} \text{ source} \tag{2.23}$$

τ_k depends on the shape of incoming wave (spherical, planar, etc.), sensor positions (ULA, NLA, circular, triangular, etc) and DOA angle of sources. From the Figure 2.2 τ_k can be calculated for ULA as,

$$\tau_k = (k-1)\frac{d\sin(\theta)}{c},\ \theta \in [-90, 90] \tag{2.24}$$

c is the propagating velocity of wave (acoustic, electromagnetic) and d is distance between sensors.

Define a new variable ω_s as,

$$\omega_s = \omega_c \frac{d\sin(\theta)}{c} \tag{2.25}$$

so the steering vector can be rewritten as,

$$\mathbf{a}(\theta) = [1,\ e^{-j\omega_s 1} \cdots, e^{-j\omega_s (\mathrm{N}-1)}]^T \tag{2.26}$$

This is analogous to time domain sampler. So, in order to avoid aliasing Nyquist sampling theorem should be considered.

$$
\begin{aligned}
|\omega_s| &\leq \pi && (2.27)\\
\left|\omega_c \frac{d\sin(\theta)}{c}\right| &\leq \pi && (2.28)\\
\left|2\pi f \frac{d\sin(\theta)}{c}\right| &\leq \pi && (2.29)\\
\left|\frac{d\sin(\theta)}{\lambda}\right| &\leq \frac{1}{2} && (2.30)\\
d|\sin(\theta)| &\leq \frac{\lambda}{2} && (2.31)\\
d &\leq \frac{\lambda}{2},\ \theta \in [-90, 90] && (2.32)
\end{aligned}
$$

d can be called as spatial sampling period. It should be smaller than the half of the incoming wavelength.

Note that this rule can be loosen if one can be sure that incoming signals DOA angles are limited in narrower region than $[-90, 90]$, if it is $[-\theta_*, \theta_*]$ value of d increases as follows,

$$d \leq \frac{\lambda}{2|\sin(\theta)|},\ \theta \in [-\theta_*, \theta_*] \quad (2.33)$$

This information is useful especially in estimation of Signal Parameters via Rotational Invariance Technique (ESPRIT).

2.2 Algorithms

Although root-MUSIC algorithm is the primary subject of this thesis, other DOA estimation algorithms, beamforming, Capon, Spectral MUSIC, ESPRIT, are introduced in basic level just to give an insight of common types of DOA estimation algorithms.

Note that all algorithms run on a DSP board or in a computer, so finite data estimates of covariance matrices require sampled data. Therefore it is assumed that sampling operation is completed and all signals used for construction of covariance matrix estimates are in discrete domain. Instead of variable t, variable n is used when required.

2.2.1 Non-Parametric Algorithms

Non-parametric DOA estimation methods do not require any restriction of covariance matrix of data. Array work as a spatial finite impulse response (FIR) filter in tapped delay line structure.

Define the tap weights as,

$$\mathbf{h} = [h_0, \ldots, h_{m-1}]^{\mathrm{T}} \tag{2.34}$$

The output of the sensors defined as,

$$\mathbf{y}(t) = \mathbf{a}(\theta)s(t) \tag{2.35}$$

Here the output of the system is

$$\mathbf{y}_F(t) = [\mathbf{h}^*\mathbf{a}(\theta)]s(t) \tag{2.36}$$

(2.36) shows that by adjusting the tap values $\{h\}_{k=1}^{m}$, $\mathbf{h}^*\mathbf{a}(\theta)$ term can be changed in order to amplify or filter out the signal coming from angle θ.

Define $\mathbf{R}$ as,

$$\mathbf{R} = \mathrm{E}\{\mathbf{y}(t)\mathbf{y}^*(t)\} \tag{2.37}$$

and power of the system output as,

$$\mathrm{E}\{|\mathbf{y}_F(t)|^2\} = \mathbf{h}^*\mathbf{R}\mathbf{h} \tag{2.38}$$

So, since $\mathbf{h}$ is adjusted for the desired θ, 2.38 gives the power of signal at that direction. By using this idea beamforming and Capon algorithms is going to be introduced in the following subsections.

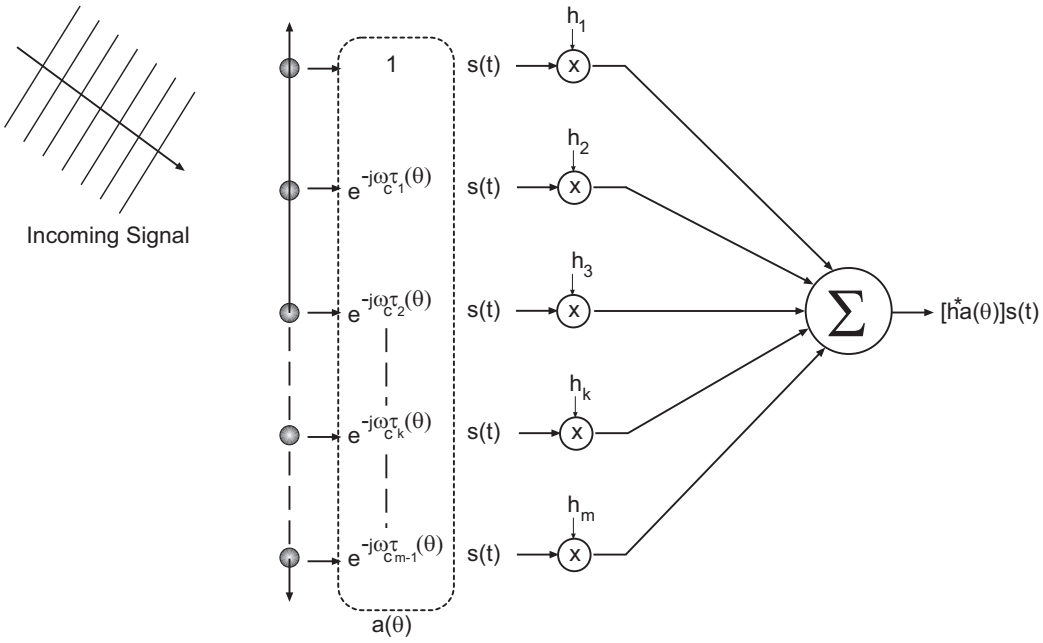

Figure 2.3: Tapped Delay Line Structure Spatial Filter

Beamforming

Beamformer design is based on following criteria,

$$\min_h \mathbf{h}^*\mathbf{h} \text{ subject to } \mathbf{h}^*\mathbf{a}(\theta) = 1 \tag{2.39}$$

while $\mathbf{a}(\theta)$ is normalized as,

$$\mathbf{a}^*(\theta)\mathbf{a}(\theta) = m \tag{2.40}$$

$\mathbf{y}(n)$ is assumed to be spatially white, i.e.

$$\mathrm{E}\{\mathbf{y}(t)\mathbf{y}^*(t)\} = \mathbf{R} = \mathbf{I} \tag{2.41}$$

so

$$\mathrm{E}\{|\mathbf{y}_F(t)|^2\} = \mathbf{h}^*\mathbf{R}\mathbf{h} = \mathbf{h}^*\mathbf{h} \tag{2.42}$$

Hence idea is to suppress signals coming from all directions except passing the signal coming from θ undistorted. Solution to optimization problem is,

$$\mathbf{h} = \frac{\mathbf{a}(\theta)}{\mathbf{a}^*(\theta)\mathbf{a}(\theta)} \tag{2.43}$$

Inserting (2.40) into (2.43) $\mathbf{h}$ becomes,

$$\mathbf{h} = \frac{\mathbf{a}(\theta)}{m} \tag{2.44}$$

When (2.44) is inserted into (2.38),

$$\mathrm{E}\{|\mathbf{y}_F(t)|^2\} = \frac{\mathbf{a}^*(\theta)\mathbf{R}\mathbf{a}(\theta)}{m^2} \tag{2.45}$$

In practice $\mathbf{R}$ can be just estimated from the finite data as,

$$\hat{\mathbf{R}} = \frac{1}{N}\sum_{n=1}^{N}\mathbf{y}(n)\mathbf{y}^*(n) \tag{2.46}$$

where N is the number of snapshots. Since $\frac{1}{m^2}$ term is just a useless constant, "The beamforming DOA estimates are given by the locations of the n highest peak of the function,"

$$\mathbf{a}^*(\theta)\mathbf{R}\mathbf{a}(\theta) \tag{2.47}$$

Capon

Capon method uses a similar optimization constraint with beamforming method. In Capon approach $\mathbf{h}$ is found in a data dependent way while beamforming is independent of data. Capon partial filter is designed as follows,

$$\min_h \mathbf{h}^*\mathbf{R}\mathbf{h} \text{ subject to } \mathbf{h}^*\mathbf{a}(\theta) = 1 \tag{2.48}$$

So capon filter passes incoming signal coming from θ, attenuates any other signal coming from direction different than θ, while beamforming just attenuates any other angle even there is no signal out there.

Solution of 2.48 is,

$$\mathbf{h} = \frac{\mathbf{R}^{-1}\mathbf{a}(\theta)}{\mathbf{a}^{*}(\theta)\mathbf{R}^{-1}\mathbf{a}(\theta)} \tag{2.49}$$

When it is inserted into system equation, output power of $\mathbf{y}_F(n)$ is as follows,

$$\mathrm{E}\{|\mathbf{y}_F(n)|^2\} = \frac{1}{\mathbf{a}^{*}(\theta)\mathbf{R}^{-1}\mathbf{a}(\theta)} \tag{2.50}$$

By using finite sample data "Capon DOA estimates are obtained as the locations of the n largest peaks of the following function",

$$\frac{1}{\mathbf{a}^{*}(\theta)\hat{\mathbf{R}}^{-1}\mathbf{a}(\theta)} \tag{2.51}$$

2.2.2 Parametric Subspace Algorithms

Spectral MUSIC

Mathematical derivation of MUSIC algorithm is presented in this subsection. Steering vector used for constructing the steering matrix $\mathbf{A}$ is as follows,

$$\mathbf{a}(\theta) \triangleq [1 \; e^{-j\omega_s} \ldots e^{-j(m-1)\omega_s}]^T_{(m\times 1)} \tag{2.52}$$

where ω_s is defined in (2.25)

$$\mathbf{A} = [\mathbf{a}(\theta_1) \ldots \mathbf{a}(\theta_n)]_{(m\times n)} \tag{2.53}$$

m is the number of sensors. Note that matrix $\mathbf{A}$ is a Vandermonde matrix [29] which has useful properties. One of the properties that a Vandermonde matrix has is,

$$rank(\mathbf{A}) = min\{m, n\} \text{ where } \theta_k \neq \theta_p, k \neq p \tag{2.54}$$

In ULA, the case where $m \leq n$, i.e. number of sources is greater or equal than sensor number, is not applicable. But for a NLA source number can be equal or greater than sensor number. This case is defined as superior case [20].

As sensor inputs defined previously in (2.21), the covariance matrix of $\mathbf{y}(t)$ can be derived as,

$$\begin{aligned} \mathbf{R}_{m\times m} &= \mathrm{E}\{\mathbf{y}(t)\mathbf{y}^*(t)\} && (2.55)\\ &= \mathrm{E}[\mathbf{A}\mathbf{s}(t)+\mathbf{e}(t)][\mathbf{s}^*(t)\mathbf{A}^*+\mathbf{e}^*(t)] && (2.56)\\ &= \mathbf{A}\mathrm{E}\{\mathbf{s}(t)\mathbf{s}^*(t)\}\mathbf{A}^*+\sigma^2\mathrm{I} && (2.57)\end{aligned}$$

Note that,

$$\mathrm{E}\{\begin{bmatrix} s_1(t)\\ \vdots \\ s_L(t)\end{bmatrix}[s_1^*(t)\dots s_L^*(t)]\} = \begin{bmatrix}\sigma_1 & & 0\\ & \ddots & \\ 0 & & \sigma_L^2\end{bmatrix} \triangleq \mathbf{P} \qquad (2.58)$$

where

$$\begin{aligned}\mathrm{E}\{s_\ell(t)s_k^*(t)\} &= \mathrm{E}\{\alpha_\ell e^{j\varphi_\ell}e^{j\Omega_\ell n}\alpha_k e^{j\varphi_k}e^{j\Omega_k n}\} && (2.59)\\ &= \alpha_\ell\alpha_k e^{j(\Omega_\ell-\Omega_k)n}\delta_{\ell,k} && (2.60)\end{aligned}$$

As a result expression for $\mathbf{R}$ can be obtained as follows,

$$\mathbf{R} = \mathbf{A}\mathbf{P}\mathbf{A}^* + \sigma^2\mathbf{I} \qquad (2.61)$$

Since $rank(\mathbf{A}\mathbf{P}\mathbf{A}^*) = n$, $\mathbf{A}\mathbf{P}\mathbf{A}^*$ term as has n strictly positive eigenvalues, the remaining $(m-n)$ eigenvalues are all being equal to zero.

Let $\{\lambda_1 \geq \dots \geq \lambda_m\}$ be the eigenvalues of R in non-increasing order and $\{s_1,\dots,s_n\}$ be the eigenvectors of $\{\lambda_1,\dots,\lambda_n\}$ and $\{g_1,\dots,g_{m-n}\}$ be the eigenvectors of $\{\lambda_{n+1},\dots,\lambda_m\}$. Remember that $\mathrm{E}\{e(p)e(k)\} = \sigma^2\delta_{p,k}$. By uniting all of these equations,

$$\begin{aligned}\lambda_k = \tilde{\lambda}_k + \sigma^2 \quad &, \quad k = 1,\dots,m && (2.62)\\ \lambda_k > \sigma^2 \quad &, \quad k = 1,\dots,n && (2.63)\\ \lambda_k = \sigma^2 \quad &, \quad k = n+1,\dots,m && (2.64)\end{aligned}$$

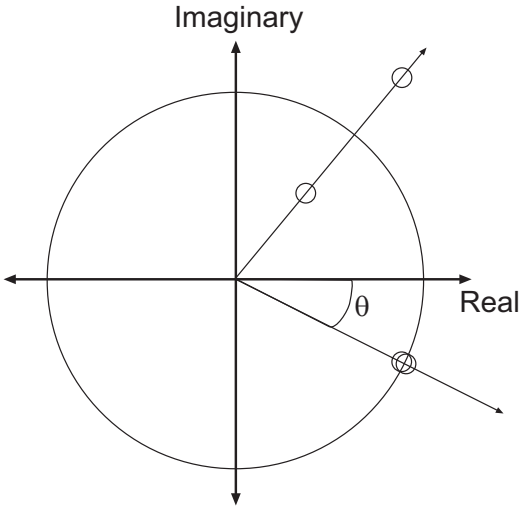

Figure 2.4: Roots of (2.73)

For these two groups of eigenvalues there are two groups of eigenvectors

$$\mathbf{S} = [\mathbf{s}_1, \ldots, \mathbf{s}_n]_{(m\times n)} \tag{2.65}$$

$$\mathbf{G} = [\mathbf{g}_1, \ldots, \mathbf{g}_{m-n}]_{(m\times(m-n))} \tag{2.66}$$

From (2.61),

$$\mathbf{RG} = \mathbf{G}\begin{bmatrix} \lambda_{n+1} & & \\ & \ddots & \\ & & \lambda_m \end{bmatrix} = \sigma^2\mathbf{G} = \mathbf{APA}^*\mathbf{G} + \sigma^2\mathbf{G} \tag{2.67}$$

$$\mathbf{APA}^*\mathbf{G} = 0 \tag{2.68}$$

Since $\mathbf{AP}$ has full rank, $\mathbf{A}^*\mathbf{G} = 0$. Mathematically column space of G is the null-space of $\mathbf{A}$

$$\mathbf{g}_k \in N(\mathbf{A}^*) \tag{2.69}$$

$$R(\mathbf{G}) = N(\mathbf{A}^*) \tag{2.70}$$

Spatial frequencies $\{\omega_k\}_{k=1}^{n}$, which are being looked for, are the only solutions of the following equation,

$$\mathbf{a}^*(\theta)\mathbf{G}\mathbf{G}^*\mathbf{a}(\theta) = 0 \quad \text{for} \quad m > n \tag{2.71}$$

This is the point where one must have to make a choice, Spectral-MUSIC or Root-MUSIC. Root-MUSIC algorithm is given in the following section continuing from this point.

DOA estimates of spectral MUSIC is the n highest peaks of function,

$$\frac{1}{\mathbf{a}^*(\theta)\mathbf{G}\mathbf{G}^*\mathbf{a}(\theta)} \tag{2.72}$$

Root MUSIC

Instead of θ in steering vector, by switching into z-domain (2.71) can be rewritten as,

$$\mathbf{a}^*(z^{-1})\mathbf{G}\mathbf{G}^*\mathbf{a}(z) = 0, \quad \mathbf{a}(z) = [1, z^{-1}, \ldots, z^{-(m-1)}]^T \tag{2.73}$$

Spatial frequency candidates are angular positions of the subset of n pairs of reciprocal solution. True solutions are the ones which are nearest to the unit circle. An example of reciprocal roots of (2.73) for two sensors and one source is given in Figure 2.4. Here the angular value of the root that is closest to the unit circle is given as θ. DOA of angle can be calculated by using (2.25).

ESPRIT

ESPRIT can only be used when array has two identical subarrays which are departed from each other by a known displacement vector Δ [15]. An example of six sensor with two subarrays consisting of four sensors of each is given in Figure 2.5.

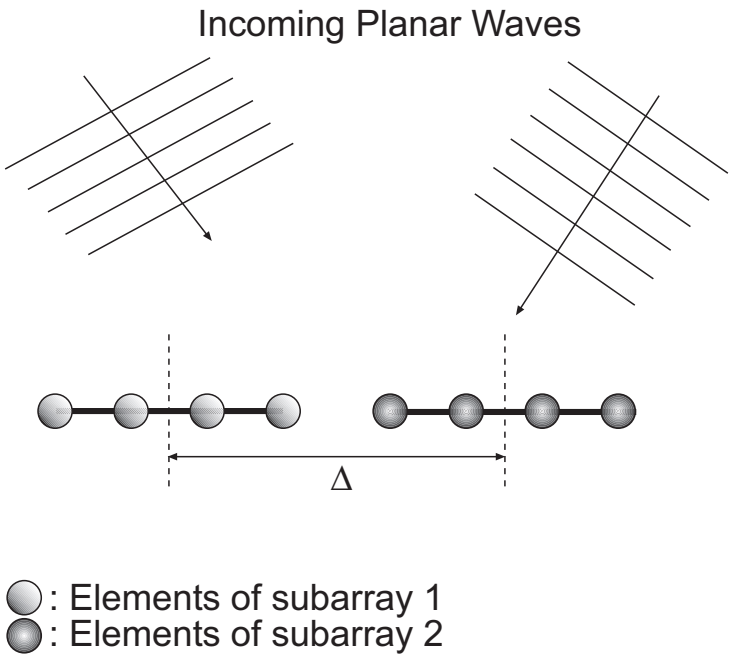

Figure 2.5: Sensors Positioned Suitable for ESPRIT Algorithm

Steering matrix $\mathbf{A}$ is parted into two matrix $\mathbf{A_1}, \mathbf{A_2}$ as,

$$\mathbf{A} = \begin{bmatrix} \mathbf{A_1} \\ \mathbf{A_2} \end{bmatrix} \tag{2.74}$$

$$\mathbf{A_1} = \begin{bmatrix} e^{-j\omega_0\tau_{11}} & \dots & e^{-j\omega_0\tau_{1L}} \\ \vdots & \ddots & \vdots \\ e^{-j\omega_0\tau_{m1}} & \dots & e^{-j\omega_0\tau_{mL}} \end{bmatrix} \tag{2.75}$$

$$\mathbf{A_2} = \begin{bmatrix} e^{-j\omega_0\tau_{\acute{1}1}} & \dots & e^{-j\omega_0\tau_{\acute{1}L}} \\ \vdots & \ddots & \vdots \\ e^{-j\omega_0\tau_{\acute{m}1}} & \dots & e^{-j\omega_0\tau_{\acute{m}L}} \end{bmatrix} \tag{2.76}$$

$$\mathbf{A_2} = \mathbf{A_1}\mathbf{D} \tag{2.77}$$

Note that $\tau_{\acute{m}\ell} = \tau_{m\ell} + \frac{\Delta\cos(\theta_\ell)}{c}$. Therefore $\mathbf{D}$ can be found as follows,

$$\mathbf{D}_{L\times L} = diag\left(e^{-j\omega_0\Delta\frac{\cos(\theta_1)}{c}}, \ldots, e^{-j\omega_0\Delta\frac{\cos(\theta_\ell)}{c}}\right) \tag{2.78}$$

$\mathbf{D}$ has L eigenvalues denoted as $\Gamma_\ell, \ell = 1, \ldots, L$

$$arg(\Gamma_\ell) = -\omega_0\Delta\frac{\cos(\theta_\ell)}{c} \tag{2.79}$$

Therefore $\{\theta_\ell\}_{\ell=1}^{L}$ can be determined from (2.79).

Unfortunately there is no explicit knowledge of $\mathbf{A_1}, \mathbf{A_2}$ and $\mathbf{D}$. Instead, from the singular value decomposition (SVD) of incoming data correlation matrix estimate S, i.e. the eigenvector estimation of signal space, can be obtained.

$$\mathbf{S} = \begin{bmatrix} \mathbf{S_1} \\ \mathbf{S_2} \end{bmatrix} \tag{2.80}$$

To find eigenvalues of $\mathbf{D}$

$$\mathbf{RS} = \mathbf{S}\begin{bmatrix} \lambda_1 & \ldots & 0 \\ \vdots & \ddots & \vdots \\ 0 & \ldots & \lambda_n \end{bmatrix} = \mathbf{APA}^*\mathbf{S} + \sigma^2\mathbf{S} \tag{2.81}$$

$$\mathbf{S} = \mathbf{A}(\mathbf{PA}^*\mathbf{S}\mathring{\mathbf{\Lambda}}^{-\mathbf{1}}) \text{ where } \mathring{\mathbf{\Lambda}} = \begin{bmatrix} \lambda_1 - \sigma^2 & \ldots & 0 \\ \vdots & \ddots & \vdots \\ 0 & \ldots & \lambda_n - \sigma^2 \end{bmatrix} \tag{2.82}$$

Define a new transformation matrix as,

$$\mathbf{C} \triangleq \mathbf{PA}^*\mathbf{S}\mathring{\mathbf{\Lambda}}^{-\mathbf{1}} \tag{2.83}$$

Therefore $\mathbf{S_1}$ can be written in terms of $\mathbf{S_2}$ as follows,

$$\mathbf{S_2} = \mathbf{A_2C} = \mathbf{A_1DC} = \mathbf{S_1C^{-1}DC} = \mathbf{S_1\Phi} \tag{2.84}$$

where Φ is defined as,

$$\Phi \triangleq \mathbf{C^{-1}DC} \tag{2.85}$$

Because of their Vandermonde structure, $\mathbf{A_1}$ and $\mathbf{A_2}$ are of full column rank. Hence $\mathbf{S_1}$ and $\mathbf{S_2}$ are full column rank. As a result Φ can be uniquely defined as,

$$\Phi = ((\mathbf{S_1^*S_1})^{-\mathbf{1}}\mathbf{S_1S_2} \tag{2.86}$$

Since Φ can obtained from $\mathbf{D}$ by a similarity transformation (2.85), Φ and $\mathbf{D}$ have the same eigenvalues. Arguments of those eigenvalues contain the angle of arrival directions that can extracted from (2.79).

2.2.3 Cramer-Rao Lower Bound

Several studies were conducted about CRB of DOA estimation algorithms [31], [32], [33], [34], [35], [36]. Closed form of CRB for DOA algorithms that is used in the simulations was derived in [19]. This is a simple closed form expression for $\mathbf{CRB}(\theta)$ that is used in this thesis.

Correlation matrix estimate $\mathbf{R}$ and steering matrix $\mathbf{A}$ are as they are in (2.61) and (2.20). $\mathbf{P}$ is the signal covariance matrix, σ is the variance of the sensor noises and N is the number of snapshots.

Define unknown variable vector $\boldsymbol{\theta}$ (arrival angles of incoming signals) as,

$$\boldsymbol{\theta} \triangleq [\theta_1, \ldots, \theta_n]^T \tag{2.87}$$

$\mathbf{D}$ is defined as,

$$\mathbf{D} = [\mathbf{d}_1, \ldots, \mathbf{d}_n] \text{ where } \mathbf{d}_k = \frac{d\mathbf{a}(\theta_k)}{d\theta_k} \tag{2.88}$$

and $\mathbf{\Pi}_A^{\perp}$ is defined as,

$$\mathbf{\Pi}_A^{\perp} = \mathbf{I} - \mathbf{\Pi}_A \text{ where } \mathbf{\Pi}_A = \mathbf{A}(\mathbf{A}^*\mathbf{A})^{-1}\mathbf{A}^* \tag{2.89}$$

According to [37] depending on the signal $s(t)$ analysis splits into two directions.

Det: $\{s(t)\}$ is a deterministic, unknown sequence

Sto: $\{s(t)\}$ is a random sequence that is circularly Gaussian Distributed with mean zero and covariance,

$$\mathrm{E}\{\mathbf{s}(t)\mathbf{s}^*(\tau)\} = \mathbf{P}\delta_{t,\tau} \tag{2.90}$$

$\hat{\mathbf{P}}$ is finite data estimate of $\mathbf{P}$ as follows where N is the number of snapshots,

$$\hat{\mathbf{P}} = \frac{1}{N}\sum_{t=1}^{N}\mathbf{s}(t)\mathbf{s}^*(t) \tag{2.91}$$

By using the notation defined above $\mathbf{CRB}_{\mathrm{Det}}(\theta)$ and $\mathbf{CRB}_{\mathrm{Sto}}(\theta)$ derived as follows.

$$\mathbf{CRB}_{\mathrm{Det}}(\theta) = \frac{\sigma}{2\mathrm{N}}\{Re(\mathbf{D}^*\mathbf{\Pi}_A^{\perp}\mathbf{D}) \odot \hat{\mathbf{P}}^{\mathrm{T}}\}^{-1} \tag{2.92}$$

$$\mathbf{CRB}_{\mathrm{Sto}}(\theta) = \frac{\sigma}{2\mathrm{N}}\{Re(\mathbf{D}^*\mathbf{\Pi}_A^{\perp}\mathbf{D}) \odot (\mathbf{P}\mathbf{A}^*\mathbf{R}^{-\mathbf{1}}\mathbf{A}\mathbf{P})^{\mathrm{T}}\}^{-1} \tag{2.93}$$

where $\odot$ is the Hadamard-Shur product.

Although the signal is finite sequence it was created on the basis of circularly Gaussian Distributed and in order to make comparison with different graphics, reference graph i.e. CRB should not change with different incoming data of each simulation. Hence in the simulations, stochastic CRB is preferred to be used.

CHAPTER 3

DOA ESTIMATION WITH NLA

In subspace methods main interest is the sample correlation matrix of the sensor data. Once the correlation matrix obtained, algorithms may immediately be applied without any further information about incoming signals. Ideally this correlation matrix should be positive definite (p.d.) Toeplitz and Hermitian Symmetric. Therefore knowing the one row of this correlation matrix theoretically should be sufficient for purposes of this discussion but in practical cases it is not. Nevertheless it may be sufficient to estimate one row, by conducting some operations on the available data.

In order to serve our purposes in this chapter, first the term co-array is explained with various examples. Second, the types of linear arrays are introduced along with their corresponding co-arrays. In last section, methods available to use NLA in DOA estimation are given.

3.1 Co-Array

Assume an N element ULA. All possible pairings of elements are listed in Table 3.1.

Total number of pairings is $\frac{N(N-1)}{2}$ as seen from summation of first column in Table 3.1. In order to express number of available pairings of an array a concept 'co-array', which was first used by Haubrich [38], is used.

Co-array shows the recurrence number of each lag in a correlation matrix. In Figure 3.1 a graphical example of a NLA is given, where sensor positions

Recurrence of Lag	Lag Distance
N	0
N-1	1
N-2	2
⋮	⋮
1	N-1

Table 3.1: Recurrence of Lags

are defined as $d_6 = [0, 1, 4, 10, 15, 17]$.

In Figure 3.1 numbers on the arrows indicate the distance between that pair of sensors. Note that distances 8 and 12 do not exist in Figure 3.1. Those are the missing covariance lags. Another important thing is all lags occurred only once, except the lags that do not ever occur. This type of array is classified as non-redundant linear array later in this chapter.

Note that the value co-array at lag zero is equal to number of sensors in array. An example of co-array for ULA is given in Figure 3.3.

Some more examples on co-array are given, as new types of NLA introduced, later in this chapter.

3.2 Array Types

Arrays can be classified according to structures of their co-arrays. Mainly there are two points to consider, gaps (holes) and redundancies in co-array. In Figure 3.2, lags 8 and 12 are the two gaps of corresponding co-array. Redundancies are elements of co-array that occur more than once.

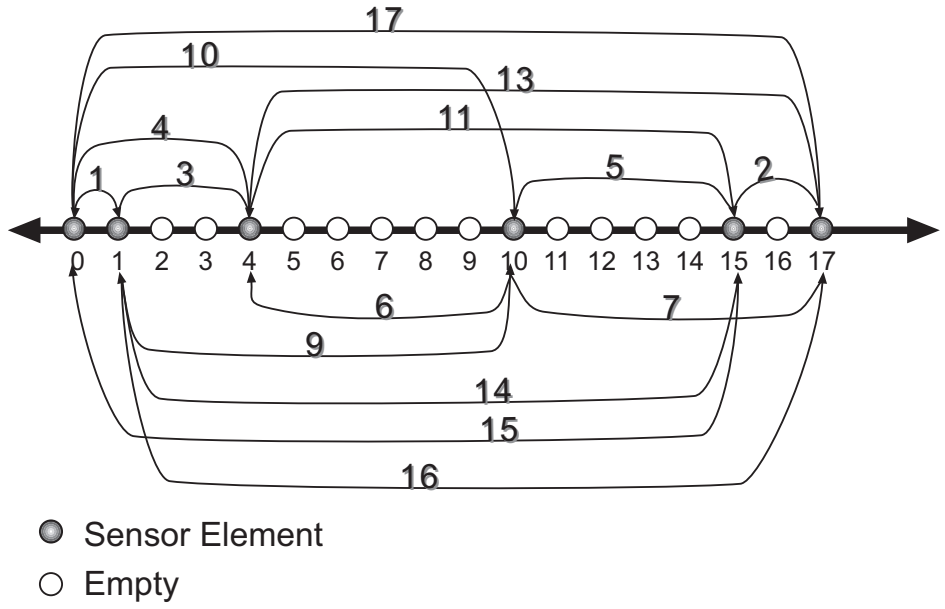

Figure 3.1: NLA with Corresponding Inter-Element Distances

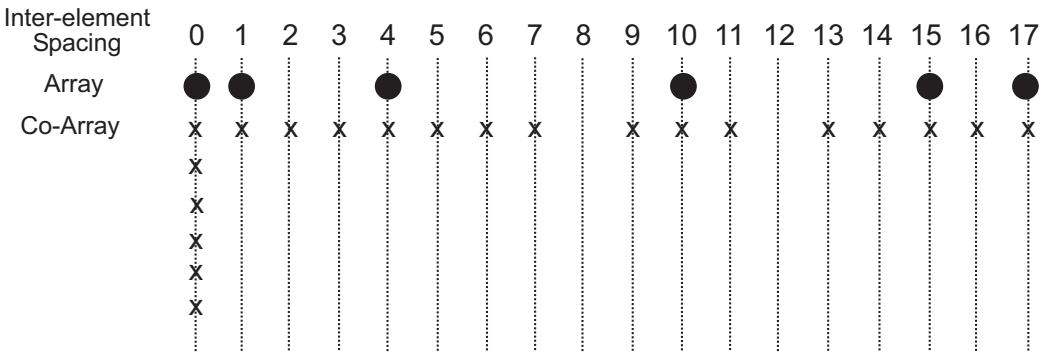

Figure 3.2: Co-Array Scheme

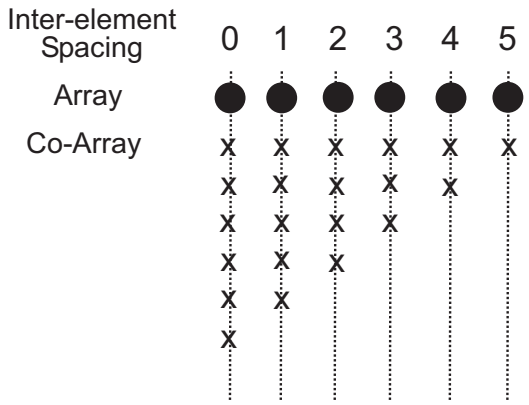

Figure 3.3: Co-Array Scheme ULA

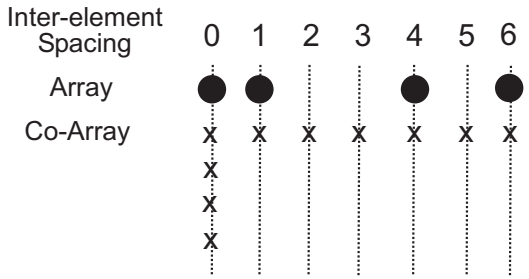

Figure 3.4: Co-Array Scheme Optimum NLA

3.2.1 Optimum Arrays

Optimum array is defined as array which has a co-array that has no gaps and no redundancy except at zero lag. This kind of array is available only up to four element sensor arrays. For more than four sensors there are only suboptimum arrays. An example of an optimum array is in Figure 3.4.

3.2.2 Sub-Optimum Arrays

Suboptimum arrays have either some gaps or redundant elements or both gaps and redundant elements. Leech [39] defined minimum redundant arrays as "redundancy is minimized under the constraint that the structure still

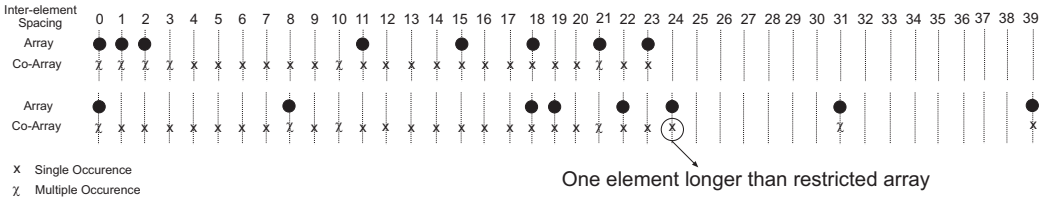

Figure 3.5: Co-Array on top is a restricted minimum redundant array, co-array at bottom is an unrestricted minimum redundant array.

provides a co-array that is contiguous″.

Non-redundant arrays as its name implies there is no redundant element in the co-array, but as its definition, this does not have strict structure. Actually by saying non-redundant arrays, optimum non-redundant arrays are implied which has the `minimum-hole´constraint besides `no redundancy´ constraint.

Min Redundant Arrays

Definition of Leech [39] results in two further subclasses. If gaps are not allowed in co-array, this type of arrays is called restricted minimum redundant arrays. If the maximum number of contiguous estimates are required, while the gaps in co-array allowed, this type of minimum redundant arrays are called unrestricted minimum redundant arrays. This two subclasses of arrays, introduced in Leech [39], are illustrated in Figure 3.5. A short version of Leech's minimum redundant array is given in Table 3.2. M is the number of sensor elements and d is the positions of sensor elements.

Non-Redundant Arrays

As defined earlier non-redundant arrays have minimum number of gaps while keeping the redundancy zero. In our discussion, these kinds of arrays are the ones, those missing co-array values are to be interpolated. An example

Table 3.2: Summary of Leech's Suboptimal Min-Redundant Sequences

M	d										
Restricted											
5	0	1	4	7	9						
6	0	1	2	6	10	13					
7	0	1	2	6	10	14	17				
8	0	1	2	11	15	18	21	23			
9	0	1	2	14	18	21	24	27	29		
10	0	1	3	6	13	20	27	31	35	36	
11	0	1	3	6	13	20	27	34	38	42	43
Unrestricted											
5	0	3	4	9	11						
6	0	4	5	6	13	16					
7	0	6	9	10	17	22	24				
8	0	8	18	19	22	24	31	39			
9	0	1	2	14	18	21	24	27	29		
10	0	16	17	28	36	42	46	49	51	73	
11	0	18	19	22	31	42	48	56	58	63	91

of non-redundant array and its co-array is given in Figure 3.2. More detailed list is provided by Sverdlik [40]. A part of his list is given in Table 3.3. M is the number of sensor elements and d is the positions of sensor elements.

Additional information should be added here, in order to be used in next chapter, where line interpolation methods are used. For the sake of interpolation there is difference between interpolating two consecutive gaps and two gaps apart from each other. For the sensor number of six, two non-redundant arrays are illustrated in Figure 3.6. Array on the top has two consecutive

Table 3.3: Summary of Sverdlik's Suboptimal Non-Redundant Sequences

M	d										
3	0	1	3								
4	0	1	4	6							
5	0	3	4	9	11						
6	0	1	4	10	12	17					
7	0	1	4	10	18	23	25				
8	0	7	10	16	18	30	31	35			
9	0	2	10	24	25	29	36	42	45		
10	0	1	6	10	23	26	34	41	53	55	
11	0	3	14	16	20	41	48	53	63	71	72
12	0	2	6	24	29	40	43	55	68	75	76	85

gaps while array in bottom has two gaps apart from each other. Although arrays in Figure 3.6 has the same number of sensors and designed with the same criterions it requires attention to make a choice between them because they perform quite differently during the line interpolation process.

3.3 Covariance Matrix Augmentation Methods

Before starting the matrix augmentation methods, it is useful to classify arrays as Abramovich [21] did. This classification is useful for deciding which type of augmentation method to choose.

There are two main groups of this classification. First one is fully augmentable arrays. Second one is partially augmentable arrays. In fully augmentable arrays co-array has no missing values, i.e. there are no gaps. There

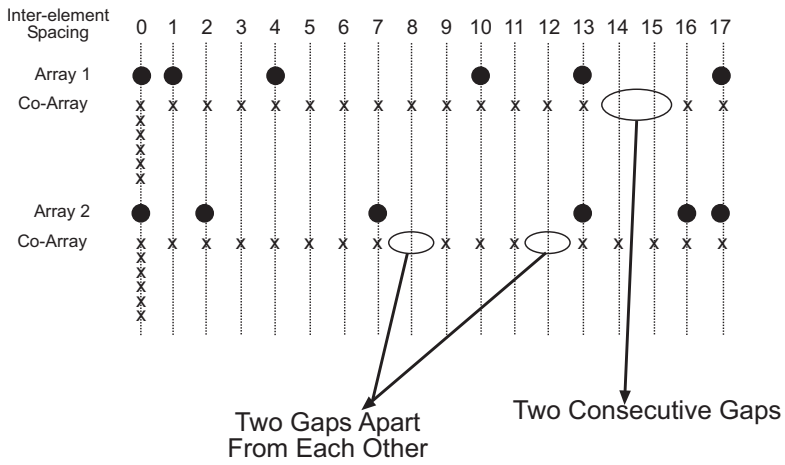

Figure 3.6: Co-Array on top is a non-redundant array with consecutive gaps, co-array at bottom is a non-redundant array with separate gaps.

may be some redundancies. Optimum arrays and restricted minimum redundancy arrays defined previously belong to this group.

For partially augmentable arrays, co-array has some missing values therefore there exist some missing diagonals in correlation matrix. Unrestricted minimum redundant arrays and non-redundant arrays are examples of this group.

3.3.1 Fully Augmentable Arrays

Theoretically correlation matrix of sensor data should be Hermitian symmetric and p.d. Toeplitz. Therefore knowing one row or every possible lag in correlation matrix is sufficient to complete it if that value is the correct one. Almost always that value is merely the average value of finite data correlation value, i.e. statistically it is not the correct value but just an estimate value.

Direct augmentation approach (DAA) [22] is a simplest way to fill correlation matrix of fully augmentable arrays but it has some drawbacks that

become obvious after mathematical derivation of DAA. Let M element NLA sensor positions are $\bar{d} = [0, d_2, d_3, \ldots, d_{\mathrm{M}}]$. D is the difference set of sensor positions defined as $D = \{d_j - d_k | j, k = 1, \ldots, \mathrm{M}; j > k\}$. d is the greatest common divisor of the set D. When measured in units of d, $\bar{d}$ can take only integer values. $d \times (M_\alpha - 1)$ is the maximum inter-element distance. κ is a natural number set defined as $\kappa = \{1, \ldots, d_{\mathrm{M}} \triangleq (M_\alpha - 1)\}$. For a co-array that has no gaps (holes) $\kappa d \in D$, i.e. that NLA has complete set of covariance lags. d_{M} variate Toeplitz covariance matrix is $\mathbf{T} = \mathrm{Toep}[t_{\kappa=i-j}]_{\kappa=0}^{d_{\mathrm{M}}}$. Let,

$$S = \kappa : \hat{t}_\kappa \text{ is specified} \tag{3.1}$$

$$\bar{S} = \kappa : \hat{t}_\kappa \text{ is unspecified} \tag{3.2}$$

t_κ ($\kappa \in S$) is obtained via DAA as,

$$\hat{t}_{j-k=\kappa} = \frac{\sum_{j,k=1}^{\mathrm{M}} \mathbf{R}_{jk} \delta(\kappa, d_j - d_k)}{\sum_{j,k=1}^{\mathrm{M}} \delta(\kappa, d_j - d_k)} \tag{3.3}$$

Each diagonal has some value and that value is found by averaging available data. Since every diagonal at least has one value it is possible to augment covariance matrix fully.

But as mentioned previously there would probably be some problems about positive definiteness of $\mathbf{T}$. Assume one of the diagonal has only one value and that value is larger than the average of main diagonal due to some noise or some finite data effect. So after averaging operation that diagonal has a larger value than main diagonal. This ruins the positive definiteness of matrix. So this effect should be included or at least expected in simulations.

3.3.2 Partially Augmentable Arrays

Linear Programming

In the literature there exists only one approach to fill the correlation matrix of the partially augmentable arrays [21]. Problem formulated as an

optimization problem. Cost is defined as entropy of the correlation matrix $\mathbf{T}$, which is obtained after DAA.

$$\mathrm{H} = \frac{1}{2}\log(\det \mathbf{T}) \tag{3.4}$$

Then starting from an initial feasible point missing values are iterated. Practically finding an initial feasible point is also another problem. Ellipsoid algorithm approach was recommended in [21] and [20] for this purpose because of its simplicity and sufficient performance. Linear programming was done by Newton's method assuming that there are no local optimum points. But in stochastic case it is mentioned that convex surface is not guaranteed so instead of the global optimum point, algorithm may stop at a local optimum point.

Therefore this method possesses some difficulties. First of all, since initial correlation matrix is an estimate of real correlation matrix from a finite sample data obtained with additional noise in sensors, it may not be possible to find an initial feasible point. Another point is, algorithm may not converge to global optimum point since convexity of cost function is not guarantied. In addition to those problems, this approach requires high computational power due to nature of linear programming.

Line Interpolation Methods

This method is actually a substitute method used in our discussion to help finding an initial point. It is not always expected to give a feasible solution but it is just enough to proceed into the method proposed in this thesis.

First, correlation matrix filled with DAA and diagonals are averaged as defined in (3.3) previously. Then first row of correlation matrix is interpolated with a method such as 'spline' or some other line interpolation methods. Note that this method should not be an approximating method which also

affects the available data. After the interpolation, first row is used to construct full correlation matrix, knowing that the correlation matrix is Toeplitz and Hermitian symmetric.

This approach is computationally light but it gives just a rough estimate of missing covariance lags in correlation matrix. So using this method alone, does not give satisfactory results.

CHAPTER 4

PROPOSED METHOD

4.1 Introduction

Array interpolation technique is widely studied in literature. Array interpolation in DOA estimation is first used in [41] for high resolution estimations. Interpolation of irregular shaped two dimensional array into a desired structure such as ULA, for a known limited sector, is considered in [41]. One of the important application is to convert an array manifold to a uniform linear array (ULA) form in order to take advantage of the Vandermonde structure, which allows the use of fast subspace methods [42].

Also for wide-band incoming signals there are plenty of studies such as Friedlander did in [43]. Main idea is to create virtual array for different frequency bands by interpolating the real array structure. Then adding up all covariance matrices belong to different virtual arrays, i.e. arrays for different frequency bands and use well known subspace DOA estimation methods by eigen decomposition of this composite correlation matrix. If virtual arrays are chosen to be ULA, as in this thesis, Root-MUSIC algorithm can be directly applicable.

Array interpolation technique are further improved in [44] for bias minimization and reducing DOA mean square error. This approach is based on rotating errors and noise subspaces into optimal directions.

For all above studies a mapping matrix, which is be called $\mathbf{T}$ along this thesis, is used for interpolation the real array into synthetic array. This

mapping matrix requires the solution of a linear equation which may be ill-conditioned in certain cases [45]. A further difficulty is the requirement to define an angular sector where all the sources are assumed to be inside. As the angular sector widens, the mapping accuracy decreases due to the least-squares solution of the mapping equation. In our discussion, the above two problems are eliminated by considering first a Wiener formulation of the mapping relation. This solution improves the condition number of the mapping matrix. In addition, mapping accuracy improves for noisy observations. In order to remove the dependency on an angular sector, an initial direction-of-arrival, (DOA), estimate is used. Since the source angles are employed in the mapping matrix, the proposed approach can handle sources with arbitrary angular directions.

Covariance matrix augmentation techniques are well known in the literature [22], [20]. Direct augmentation approach (DAA) [22], has certain limitations especially for medium SNR levels [21] and it is proposed mainly for fully augmentable array structures such as restricted minimum redundancy arrays.

In this context, our focus is on the partially augmentable arrays and therefore non-redundant arrays are considered. It is possible to find locally optimum augmentation techniques [21] for such arrays but they are computationally expensive and as the number of missing covariance lags increases the search for linear programming increases. Proposed approach uses an initial estimate of the source DOA, and further improves this estimate by using the array interpolation technique. The computational complexity for this initial estimate is less than the approach in [21] is assumed and well worthed when the improvement in DOA estimation is considered. The missing covariance lags for the initial estimate can be augmented by employing a variety of approaches such as zero insertion, or spline interpolation, which is mentioned in section 3.3.2. Once this initial estimate has been obtained, this

estimate is used in the array interpolation technique to obtain a mapping matrix which returns an estimate of the full array covariance matrix when the sample covariance matrix is given.

In this thesis, the conventional case for the number of sources, namely the number of sources is less than the number of sensors, is considered. However it is possible to modify the same approach for the superior case as it is in [20] and to illustrate this case few simulation results are given in section 5.2. Several simulations have been conducted and these experiments show that the proposed approach improves the DOA estimates significantly for nonuniform linear arrays.

4.2 Problem Formulation

It is assumed that NLA has M sensors located at integer multiples of half the wavelength, $\lambda/2$, with sensor locations as d_i, $i = 1, ..., M$. Furthermore the inter-sensor distances is incomplete and L element co-array has missing covariance lags. It is assumed that the source signals, $s_k(t)$, are Gaussian distributed and they are uncorrelated. Arrival angles of sources are expressed in vector form as, $\boldsymbol{\theta} = [\theta_1, ..., \theta_n]$ where θ_k is the DOA of the k^{th} source. Then the received signal for narrowband signals can be modeled as,

$$\mathbf{y}(t) = \bar{\mathbf{A}}(\theta)\mathbf{s}(t) + \mathbf{v}(t) \tag{4.1}$$

where $\bar{\mathbf{A}}(\theta) = [\mathbf{a}(\theta_1), ..., \mathbf{a}(\theta_n)]$ is the manifold matrix for NLA, $\mathbf{s}(t)$ is the zero-mean source vector as $\mathbf{s}(t) = [s_1(t), ..., s_n(t)]^T$ and $\mathbf{v}(t)$ is the additive white Gaussian noise with $\mathbf{R_v} = \sigma_v^2\mathbf{I}$. The sample covariance matrix is given as,

$$\hat{\mathbf{R}} = \frac{1}{N}\sum_{n=1}^{N}\mathbf{y}(n)\mathbf{y}^*(n) \tag{4.2}$$

The problem is to estimate $\boldsymbol{\theta}$ given N independent snapshots. Main concentration is the DOA accuracy for NLA and focus is the improvement of

DOA estimates. The improvement on DOA estimate depends on the covariance matrix. Since we have a sparse array, it is required to find missing covariance lags and obtain the $M_\alpha \times M_\alpha$ covariance matrix estimate of the M_α-element uniform linear array. If the covariance matrix estimate is sufficiently accurate, it is expected to have a better performance compared to the conventional processing for NLA. In this respect, performance of the proposed approach with the uniform full array is compared.

4.3 Array Interpolation

In array interpolation, a mapping matrix $\mathbf{T}$ is used [41] to obtain data from a virtual uniform linear array when the data from an actual array is given . In order to have an accurate mapping (or interpolation), the number of actual sensors is usually selected larger than the virtual array elements. Furthermore mapping is devised only for an angular sector $[\theta_b, \theta_e]$ where the sources are assumed to be located. Let $\mathbf{A}_s(\tilde{\theta})$ and $\bar{\mathbf{A}}_s(\tilde{\theta})$ be the manifold matrices for the angles in the angular sector for ULA and NLA respectively. $M_\alpha \times M$ mapping matrix [42] designed for the best square fit between range spaces of these two manifold matrices is

$$\mathbf{T} = \mathbf{A}_s(\tilde{\theta})\bar{\mathbf{A}}_s(\tilde{\theta})^\dagger = \mathbf{A}_s(\tilde{\theta})\bar{\mathbf{A}}_s^*(\tilde{\theta})(\bar{\mathbf{A}}_s(\tilde{\theta})\bar{A}_s^*(\tilde{\theta}))^{-1} \tag{4.3}$$

where $\bar{\mathbf{A}}_s(\tilde{\theta})^\dagger$ is the Moore-Penrose pseudo-inverse. Both $\mathbf{A}_s(\tilde{\theta})$ and $\bar{\mathbf{A}}_s(\tilde{\theta})$ are built by dividing the angular sector $[\theta_b, \theta_e]$ into $\Delta\theta$ intervals. $\tilde{\theta}_i = i\Delta\theta$ and a source is assumed for each $\tilde{\theta}_i, i = 1, ..., \frac{\theta_e - \theta_b}{\Delta\theta} + 1$. Since $\mathbf{T}$ is found as the least squares solution, as the $\theta_e - \theta_b$ increases, the accuracy of the mapping decreases. On the other hand, there is no information regarding the source direction a priory and it is desired to keep $\theta_e - \theta_b$ as large as possible to cover the most of the looking directions. This contradiction is one of the limitations of array interpolation.

Another problem in finding $\mathbf{T}$ is the condition number of $\bar{\mathbf{A}}_s(\tilde{\theta})\bar{\mathbf{A}}_s^*(\tilde{\theta})$. This matrix may be ill-conditioned for certain angular sectors [45]. In such a case, an approximate solution is sought as in [45]. In the following part, the Wiener formulation for the solution of this problem is presented.

Given $\mathbf{y} = \bar{\mathbf{A}}(\theta)\mathbf{s} + \mathbf{v}$ of the NLA it is required to find $\hat{\mathbf{y}} = \mathbf{A}(\theta)\mathbf{s}$ of the ULA. If error defined as $\mathbf{e} = \hat{\mathbf{y}} - \mathbf{T}\mathbf{y}$ and find the MSE optimum solution for $\mathbf{T}$, following equation can be obtained,

$$\mathbf{T} = \mathbf{A}_s(\tilde{\theta})\mathbf{R}_s\bar{\mathbf{A}}_s^*(\tilde{\theta})[\bar{\mathbf{A}}_s(\tilde{\theta})\mathbf{R}_s\bar{\mathbf{A}}_s^*(\tilde{\theta}) + \mathbf{R}_v]^{-1} \tag{4.4}$$

Assuming $\mathbf{R}_s = \sigma_s^2\mathbf{I}$ and $\mathbf{R}_v = \sigma_v^2\mathbf{I}$,

$$\mathbf{T} = \sigma_s^2\mathbf{A}_s(\tilde{\theta})\bar{\mathbf{A}}_s^*(\tilde{\theta})[\sigma_s^2\bar{\mathbf{A}}_s(\tilde{\theta})\bar{\mathbf{A}}_s^*(\tilde{\theta}) + \sigma_v^2\mathbf{I}]^{-1} \tag{4.5}$$

When the mapping matrix formulations in (4.3) and (4.5) is compared, the similarities as well as the differences become obvious. The Wiener solution in (4.5) performs better at low SNR compared to (4.3). In addition, $\sigma_v^2\mathbf{I}$ in (4.5) improves the condition number of the matrix inverse and matrix inverse always exist and well-defined especially at low-to-medium SNR levels which is the range for practical applications.

4.4 Covariance Matrix Augmentation and DOA Estimation

In the previous section, array interpolation was described and the Wiener formula was presented for the mapping matrix $\mathbf{T}$. Assuming that an initial estimate for DOA $\boldsymbol{\theta} = [\theta_1, \theta_2, ..., \theta_n]$ is available, the $\mathbf{T}$ matrix is constructed by considering narrow sectors for each θ_i, namely $[\theta_i - \theta_\epsilon, \theta_i + \theta_\epsilon]$. These sectors are divided into $\frac{2\theta_\epsilon}{M_\alpha/M}$ parts or $\tilde{\theta}_i = \theta_i - \theta_\epsilon + i\frac{2M\theta_\epsilon}{M_\alpha}$. This type of construction for $\mathbf{A}_s(\tilde{\theta})$ and $\bar{\mathbf{A}}_s(\tilde{\theta})$ results full row rank matrix in order to have a well-defined pseudo-inverse.

Once $\mathbf{T}$ is constructed, $M_\alpha \times M_\alpha$ augmented covariance matrix $\mathbf{R}_a$ is estimated from the $M \times M$ sample covariance as,

$$\mathbf{R}_a = \mathbf{T}\hat{\mathbf{R}}\mathbf{T}^* \tag{4.6}$$

As the post processing step, redundancy averaging is used as in [46] to generate a Toeplitz matrix. The complete procedure in order to have an improved DOA estimate is summarized below.

Step1: Given $\mathbf{y}(n)$, estimate an augmented covariance matrix by DAA and obtain a Toeplitz matrix by redundancy averaging. As an option, use spline interpolation in order to fill the missing covariance lags.

Step2: Use the covariance matrix found in Step 1 and find an initial DOA estimate by assuming that the number of sources is known. In our case, Root-MUSIC is used for this purpose.

Step3: Given $\boldsymbol{\theta}$ from Step 2, construct $\mathbf{T}$ from (4.5) and as explained in sections 4.3 and 4.4.

Step4: Find $\mathbf{R}_a$ from (4.6) and use Root-MUSIC by employing $\mathbf{R}_a$ to find the improved DOA estimate.

CHAPTER 5

PERFORMANCE EVALUATION OF THE PROPOSED METHOD

The proposed approach for the improvement of DOA estimation in sparse arrays is implemented by considering a six element non-redundant partially augmentable NLA with sensor locations as $d_6 = [0 \quad 1 \quad 4 \quad 10 \quad 12 \quad 17]$ [21]. In order to show that different gap positions create different performances, array of $\tilde{d}_6 = [0 \quad 1 \quad 4 \quad 10 \quad 15 \quad 17]$ is used in Figure 5.21. Root-MUSIC algorithm is chosen to be the subspace algorithm that uses the augmented covariance matrix.

There are two missing covariance lags for the NLA d_6. Performance of this NLA is compared with both six and eighteen element ULAs. In addition, CRB [19] is used for these full arrays in order to see the theoretical limits for Root-MUSIC algorithm. Proposed algorithm denoted as CA-AI. Full array performances are indicated by FA-6 and FA-18 for the six and eighteen element ULA respectively. CRB plots are CRB-6 and CRB-18 for the corresponding ULA's respectively. The sources are generated equal power and they are uncorrelated with each other. Source signals are Gaussian processes and noise is a white sequence as defined in subsection 2.1.1. Each experiment is the average of 500 trials. And the number of snapshots is chosen to be 1000 unless otherwise stated.

5.1 Conventional Number of Sources

For the conventional case, subspace algorithms that use M element ULA can identify at most M − 1 uncorrelated sources. Therefore for d_6 up to five sources are considered as the conventional case. Beyond five sources, the case is called superior case which is illustrated in section 5.2.

5.1.1 One Source

Figure 5.1 shows the results of the above algorithms for a single source at 60 degrees. As it is seen from this Figure, proposed approach performs significantly better compared to the same number of ULA (namely FA-6), indeed close to the full array performance, FA-18.

In Figure 5.2 one source is swept from one endfire to other endfire. This experiment displays general angle dependent characteristics of linear arrays which has higher error at endfires, lower error at broadside.

5.1.2 Two Sources

Figure 5.3 shows the performance of the algorithms when one source is at 90 degrees (broadside) and the second source is swept from 10 to 89 degrees. SNR is set to 20 dB. The performance of the proposed approach is better than CRB-6. This result shows that the proposed approach is independent of a sector as opposed to the conventional array interpolation [45].

In Figure 5.4 and Figure 5.5, algorithms are compared for their SNR and number of snapshot performances respectively. In this case, the sources are closely located at 55 and 60 degrees respectively. The RMSE of the proposed approach begin to saturate at high SNR values because Wiener formulation lose its effect at high SNR and mapping matrix accuracy begin to decrease. This point is clarified with more simulations later in this subsection.

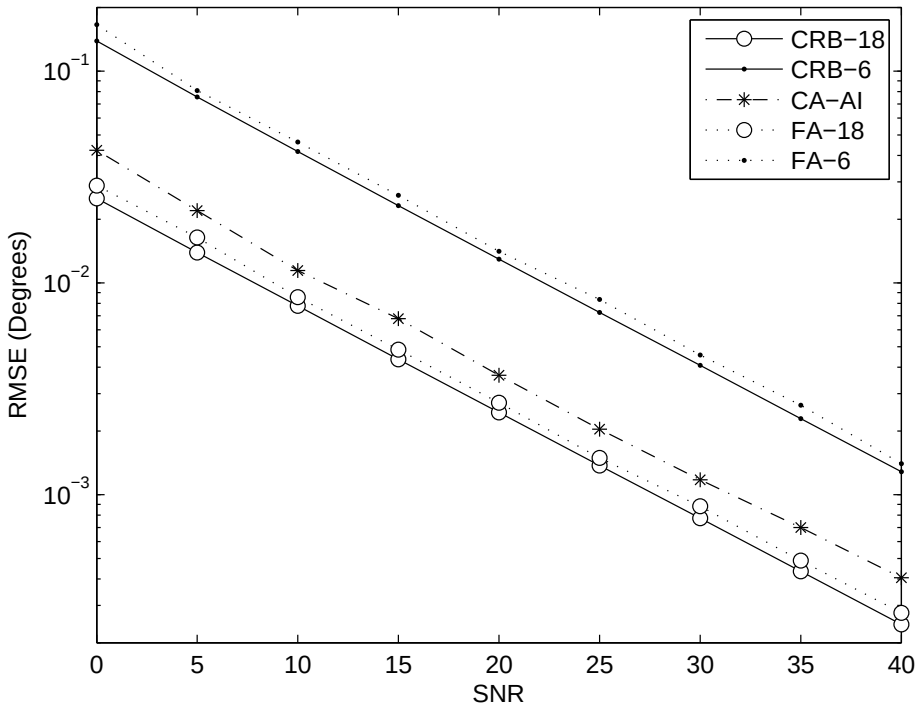

Figure 5.1: Performance for one source located at 60 degrees with increasing SNR.

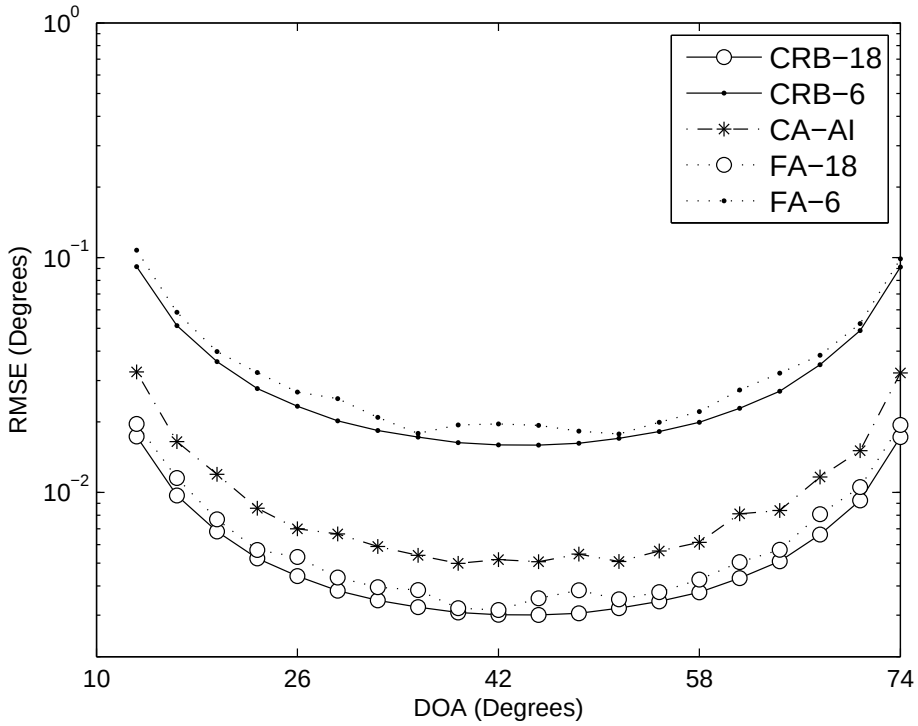

Figure 5.2: Performance for one source which is moving from 10 to 170 degrees.

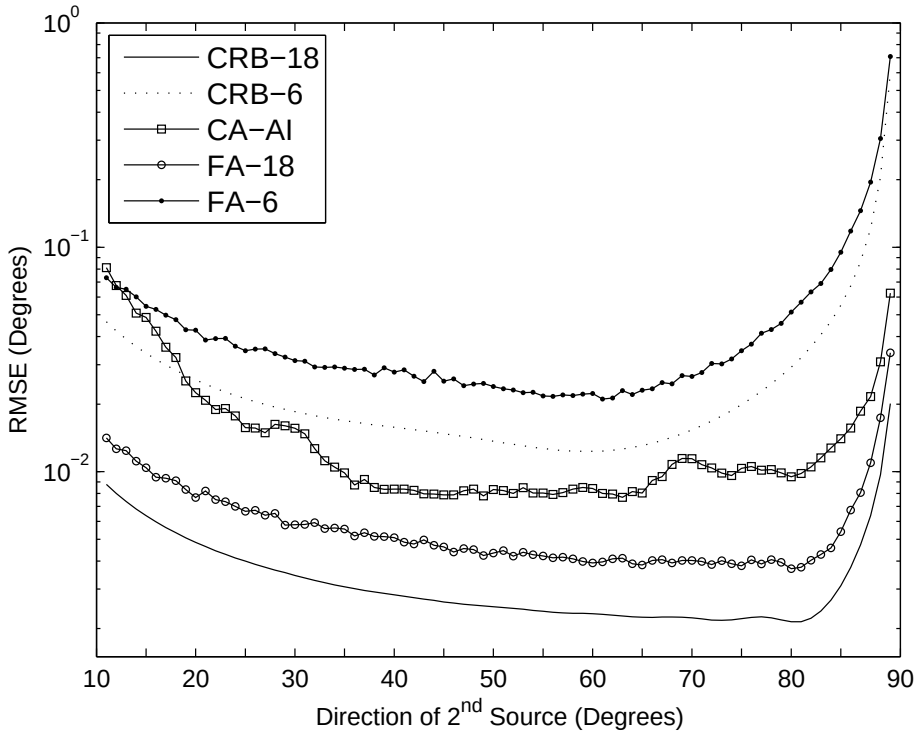

Figure 5.3: Performance when the source at 90 degrees is fixed and a second source is swept.

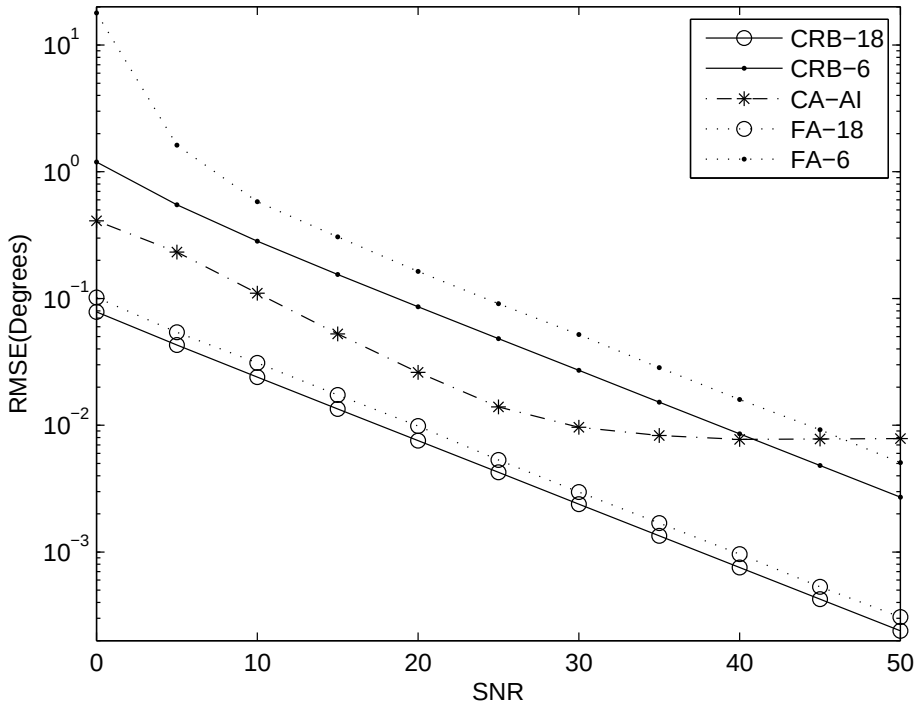

Figure 5.4: Performance of the algorithms for increasing SNR when two sources are located at 55 and 60 degrees respectively.

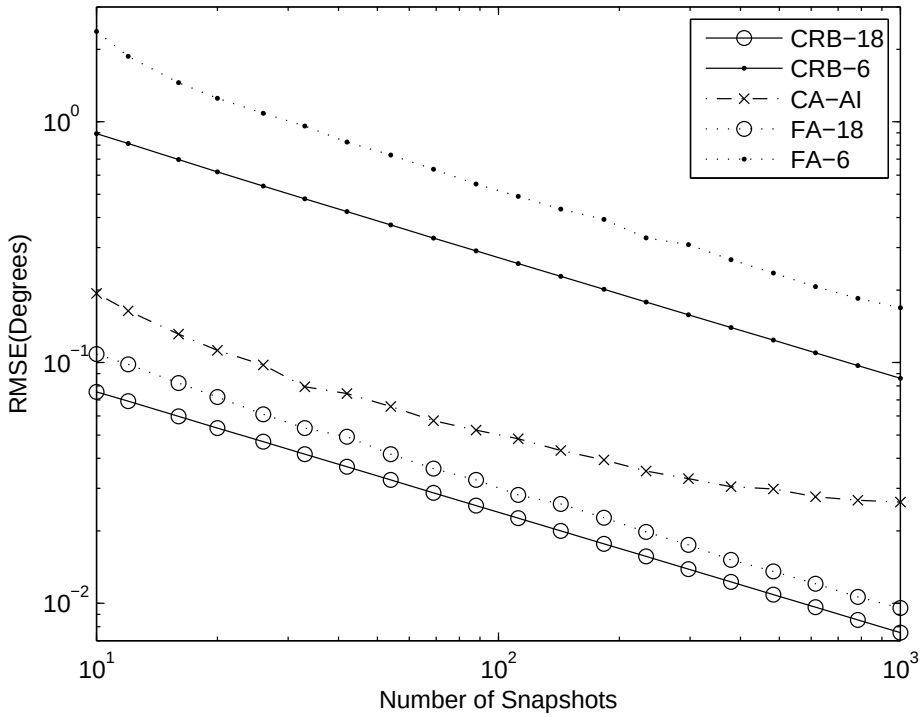

Figure 5.5: Performance of the algorithms for the number of snapshots when two sources are located at 55 and 60 degrees.

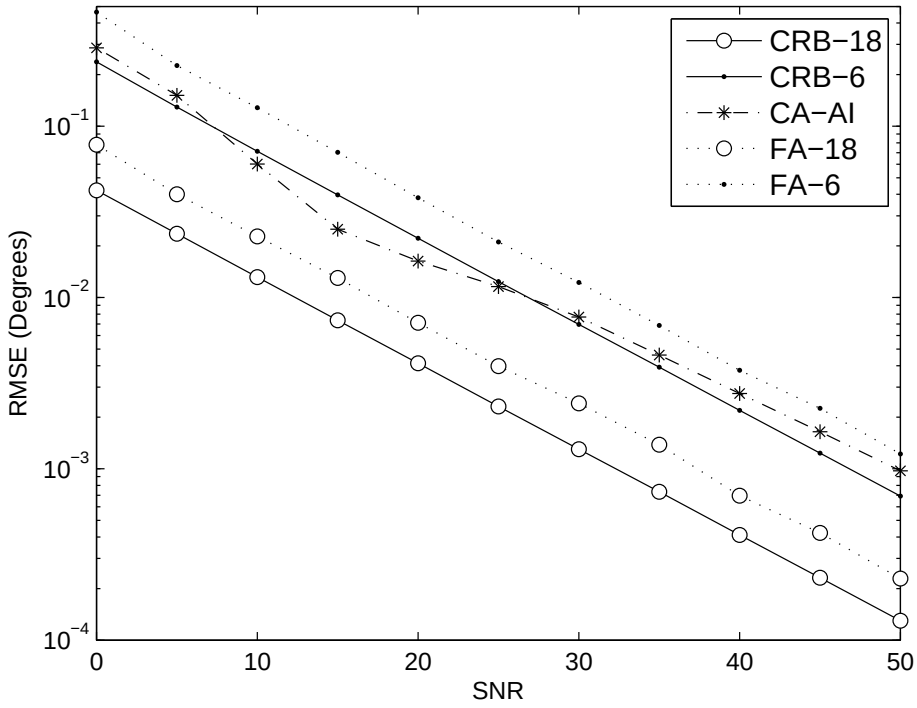

Figure 5.6: Performance for two sources located at 60 and 140 degrees with respect to increasing SNR.

Figure 5.6 and Figure 5.7 illustrate the previous two experiments with sources that are far from each other. In these graphs it is seen that interpolated array can work without angular sector limitations.

Effects of Wiener Formulation

Mapping matrix formulation in 4.5 is repeated here in order to indicate the effect of Wiener formulation with simulation results.

$$\mathbf{T} = \sigma_s^2 \mathbf{A}_s(\tilde{\theta}) \bar{\mathbf{A}}_s^*(\tilde{\theta}) [\sigma_s^2 \bar{\mathbf{A}}_s(\tilde{\theta}) \bar{\mathbf{A}}_s^*(\tilde{\theta}) + \sigma_v^2 \mathbf{I}]^{-1} \tag{5.1}$$

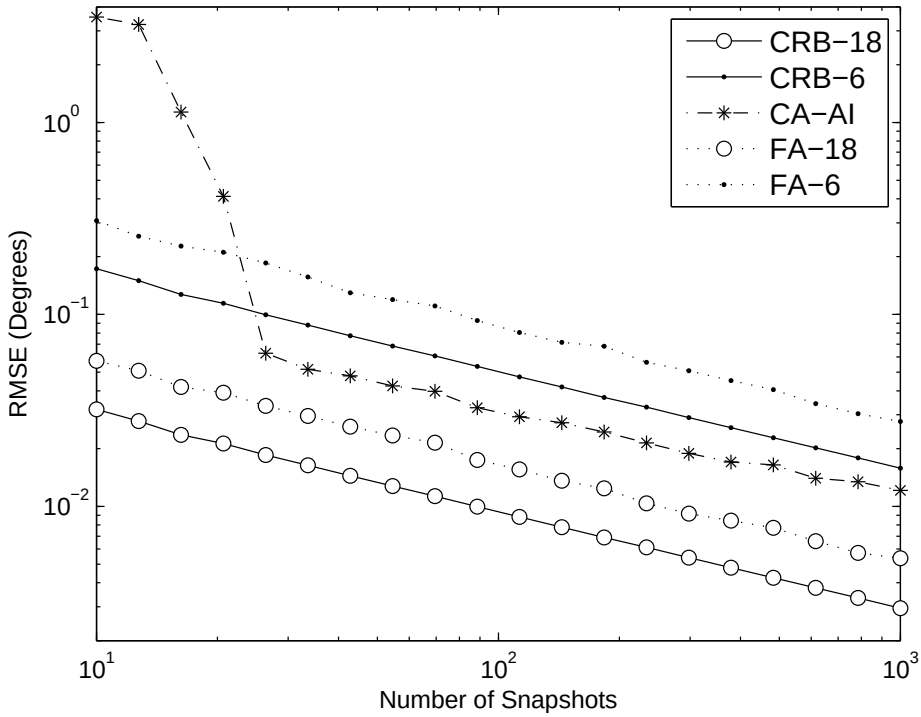

Figure 5.7: Performance for two sources located at 60 and 140 degrees with respect to increasing number of snapshots.

In Figures 5.8 and 5.9 y axis is denoted as 'condition number'. It is the condition number of the inverse term

$$\sigma_s^2 \bar{\mathbf{A}}_s(\tilde{\theta}) \bar{\mathbf{A}}_s^*(\tilde{\theta}) + \sigma_v^2 \mathbf{I} \tag{5.2}$$

taken from (5.1). If Wiener formulation is not used, inverse term should be as follows,

$$\bar{\mathbf{A}}_s(\tilde{\theta}) \bar{\mathbf{A}}_s^*(\tilde{\theta}) \tag{5.3}$$

Condition number of (5.2) indicates how well is T constructed. Therefore higher condition number cause flaws in T construction. Note that SNR is inversely related to σ^2. Increasing SNR means decreasing σ^2 so $\sigma^2\mathbf{I}$ term in (5.2) vanishes with increasing SNR values, that increases errors in the construction of $\mathbf{T}$. This is illustrated in Figure 5.8 as increasing SNR cause increasing condition number. For high SNR values condition number for Wiener formulation approaches the condition number of inverse term that does not use Wiener formulation (5.3).

In Figure 5.9 it is illustrated that condition number is not affected by the angles of sources, for the Wiener formulation.

In Figures 5.10 and 5.11 performance of proposed algorithm is shown both when $\mathbf{T}$ is constructed by Wiener formulation and Pseudo-Inverse formulation. As explained previously up to certain SNR values (around 30) Wiener formulation improves the performance. When Figure 5.11 is compared with Figure 5.9 it is seen that performance is directly related to condition number as for higher condition number, results in more error in DOA estimation. Since Wiener formulation provides much lower condition number for sensor position, performance result comes out to be source position independent.

5.1.3 Three Sources

In Figure 5.12, 5.13 and 5.14 are the simulation results of SNR and number of snapshots dependencies of three sources. They are repetition of

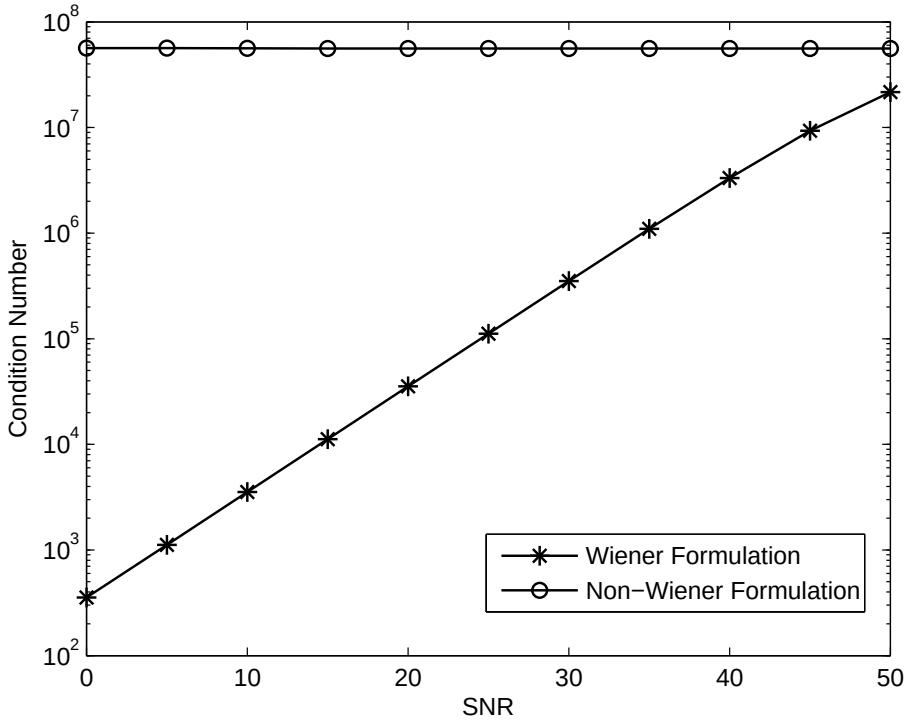

Figure 5.8: Condition Number of Inverse Term in (4.5) for two sources located at 60 and 50 degrees with respect to increasing SNR.

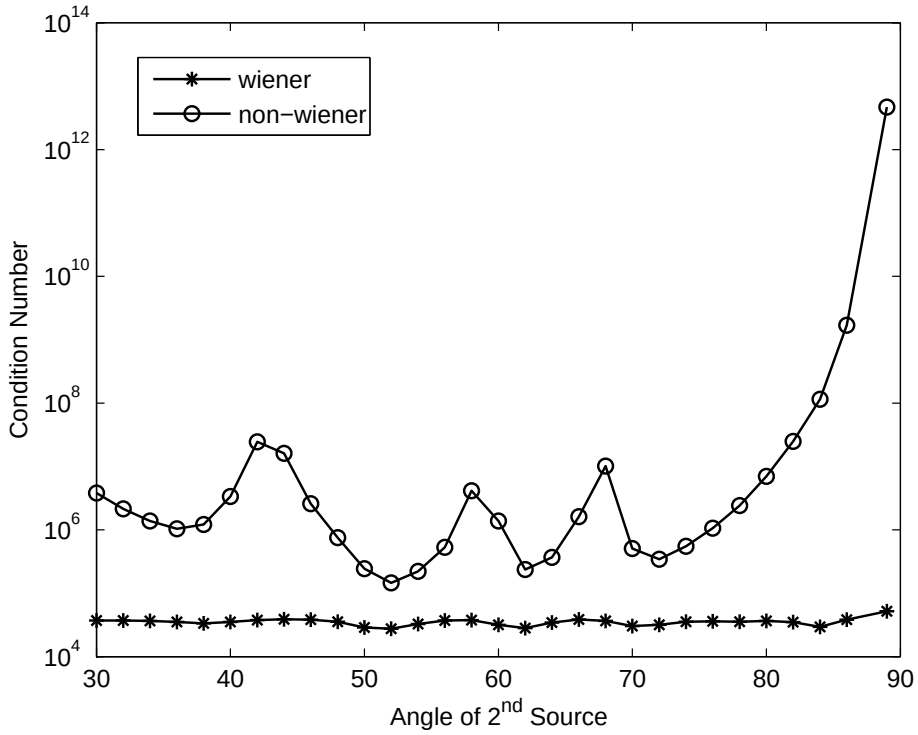

Figure 5.9: Condition Number of Inverse Term in (4.5) for one source located at 90 other source swept 30 to 89 degrees.

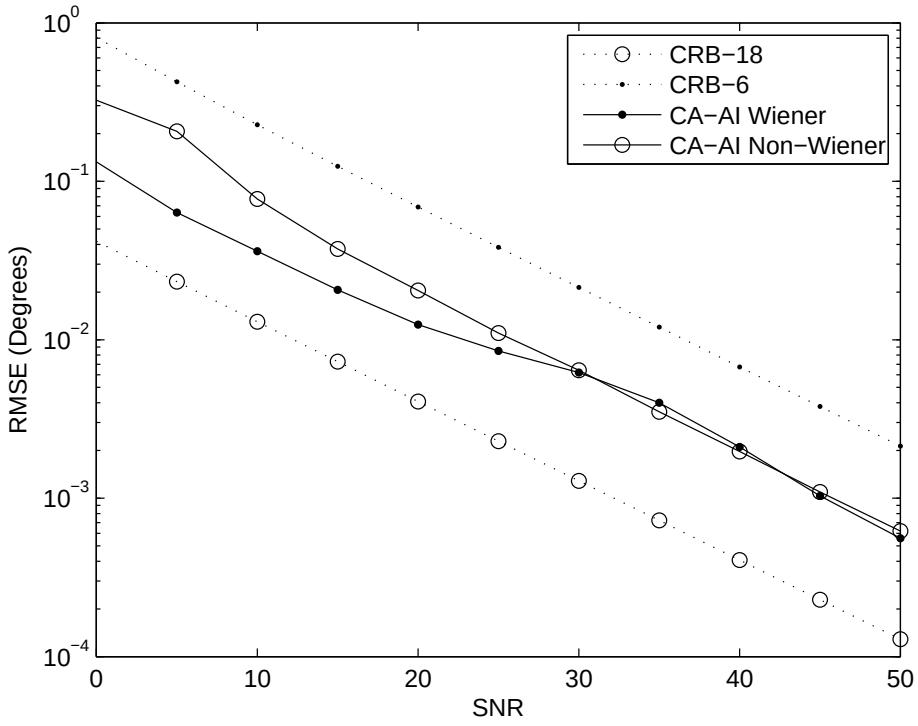

Figure 5.10: Performance of Wiener formulation for two sources located at 50 and 60 degrees with respect to increasing SNR.

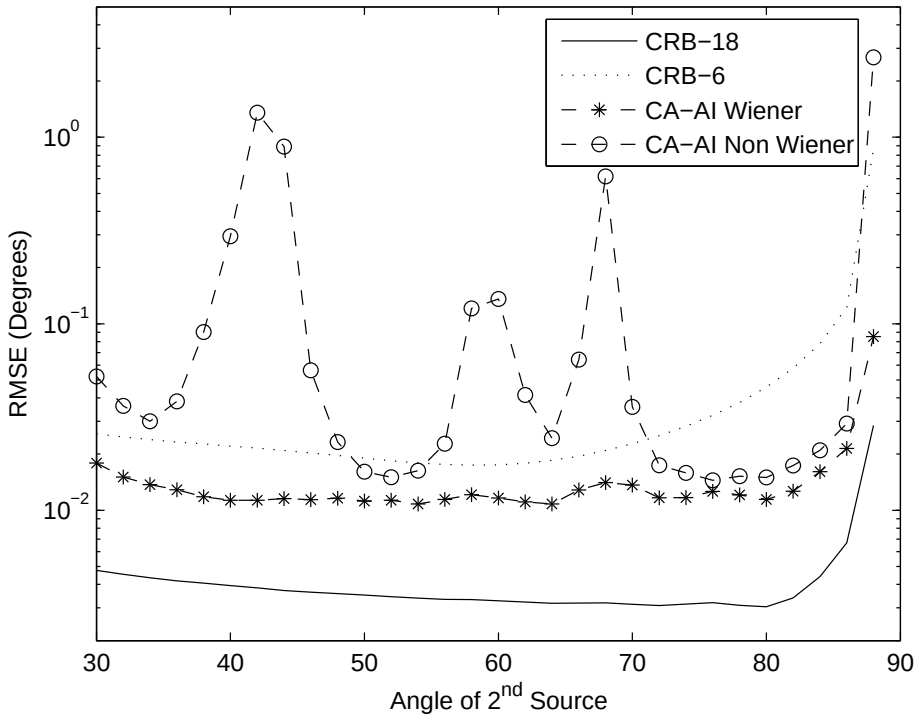

Figure 5.11: Performance of Wiener formulation for one source located at 90 other source swept 30 to 89 degrees.

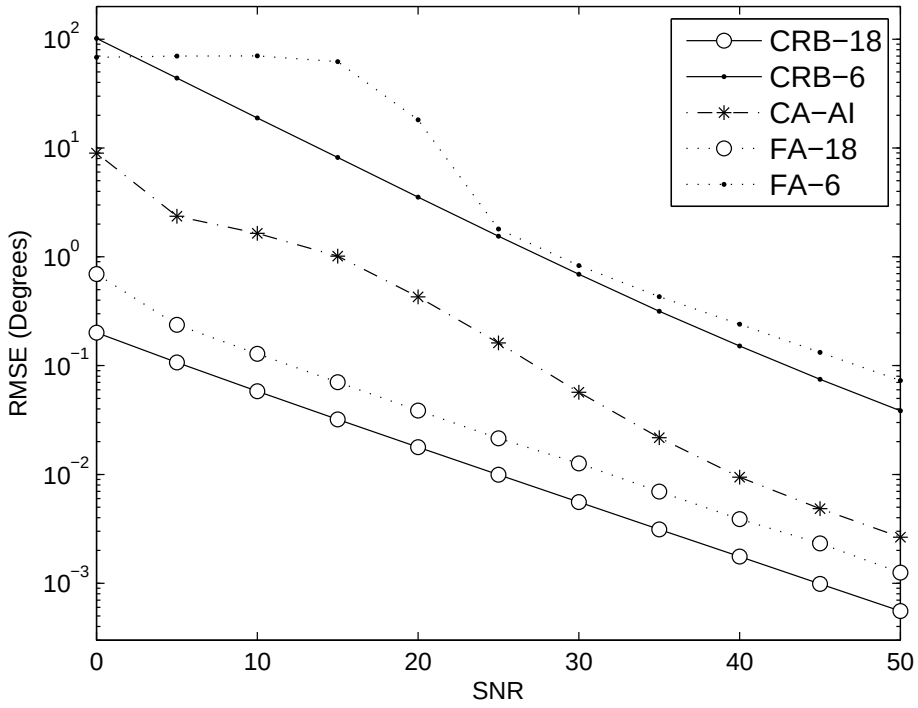

Figure 5.12: Performance for three sources located at 56, 60 and 64 degrees with respect to increasing SNR.

previous experiments for two sources. CRB, full arrays and corrected array performs the same characteristics along with upwards shift in the RMSE.

In Figure 5.14 two things can be observed at the same time. Corrected array has a successful performance with both closely spaced sources and separated sources at the same time.

5.1.4 Four Sources

In the following part, we considered four sources to indicate the sector independence as well as the performance for multiple source case. In Figure

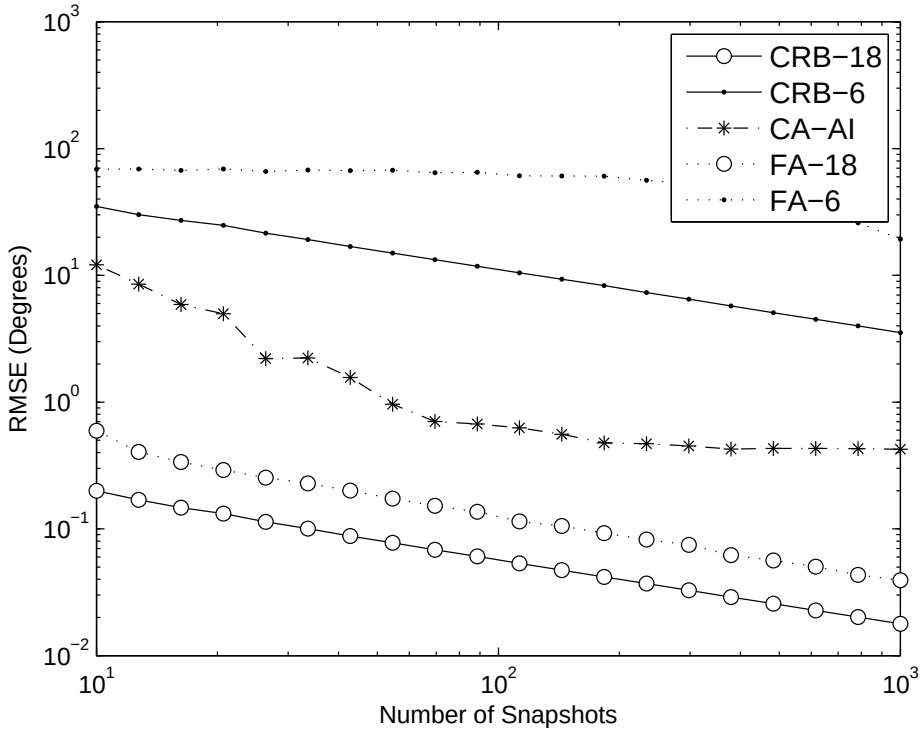

Figure 5.13: Performance for three sources located at 56, 60 and 64 degrees with respect to increasing number of snapshots.

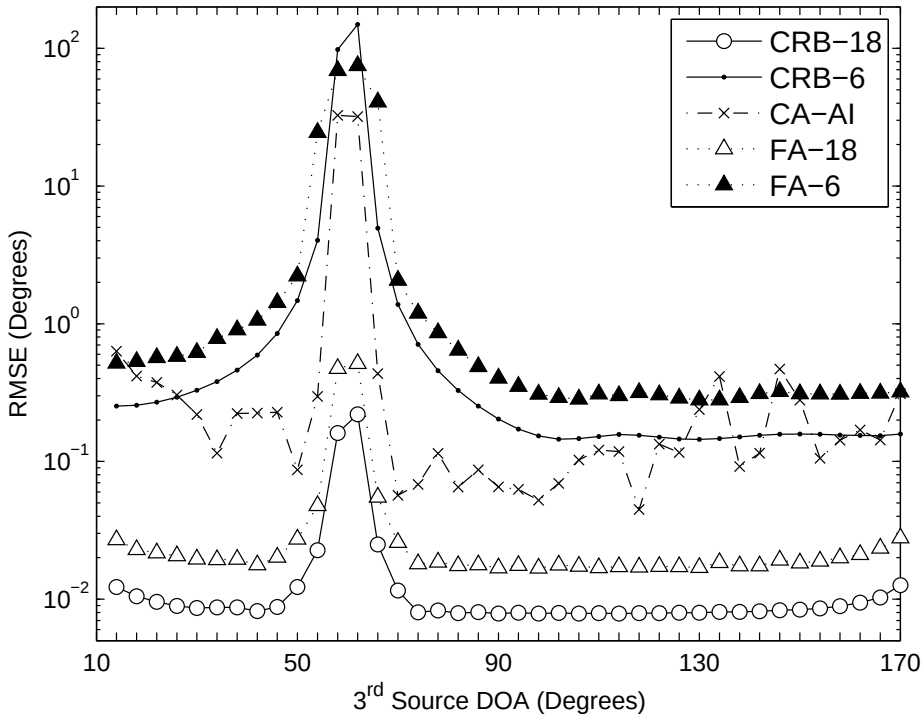

Figure 5.14: Performance for two sources located at 56 and 60 degrees, third one is moving 10 to 170 degrees.

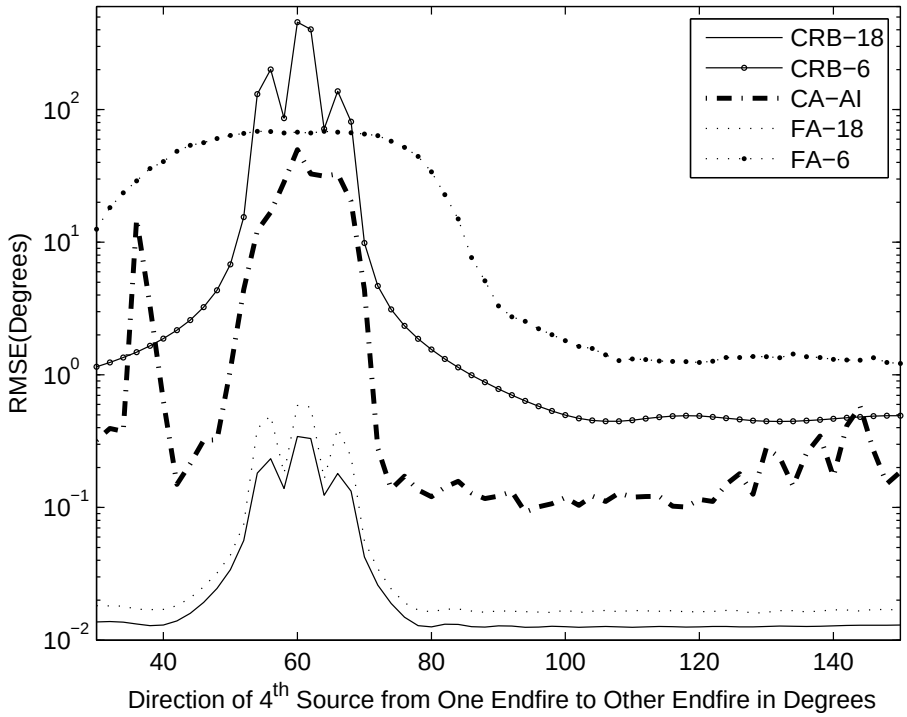

Figure 5.15: Performance of three sources fixed at 55, 61 and 67 degrees and the fourth source is swept 30 to 150 degrees.

5.15, three sources are placed at 55, 61 and 67 degrees respectively and one source is swept from 30 to 150 degrees. SNR is set to 20 dB. The performance of the proposed approach is significantly better than the FA-6 even though it is not close to FA-18. In Figure 5.15, we have the SNR performance for four sources located at 55, 60, 65 and 120 degrees respectively. As it is seen from this figure, the proposed approach improves the DOA estimates significantly and the additional complexity due to an initial estimate is well worthed.

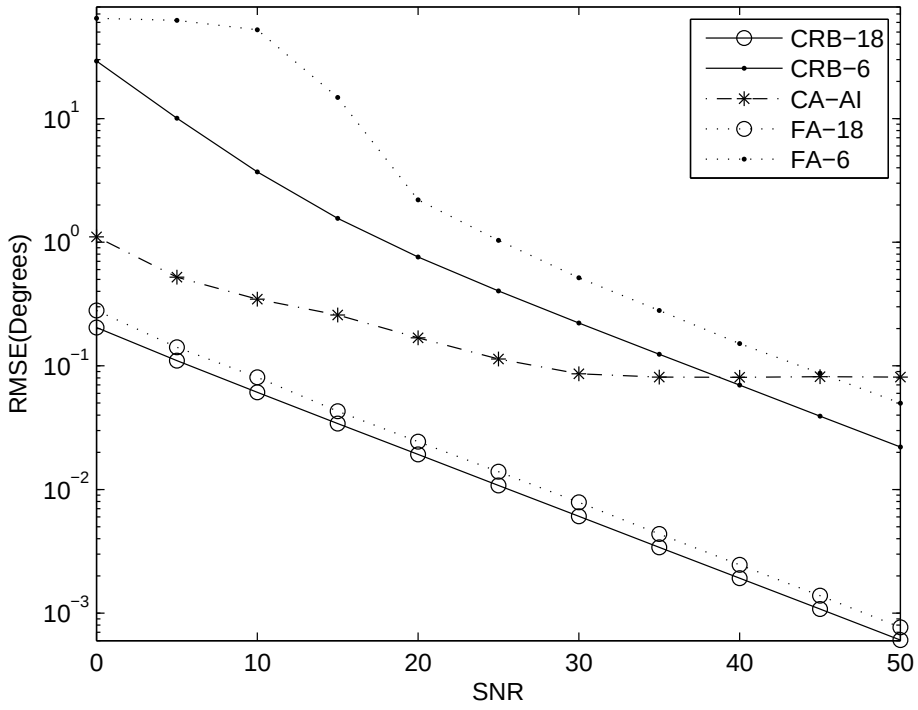

Figure 5.16: Performance for four sources located at 55, 60, 65 and 120 degrees respectively.

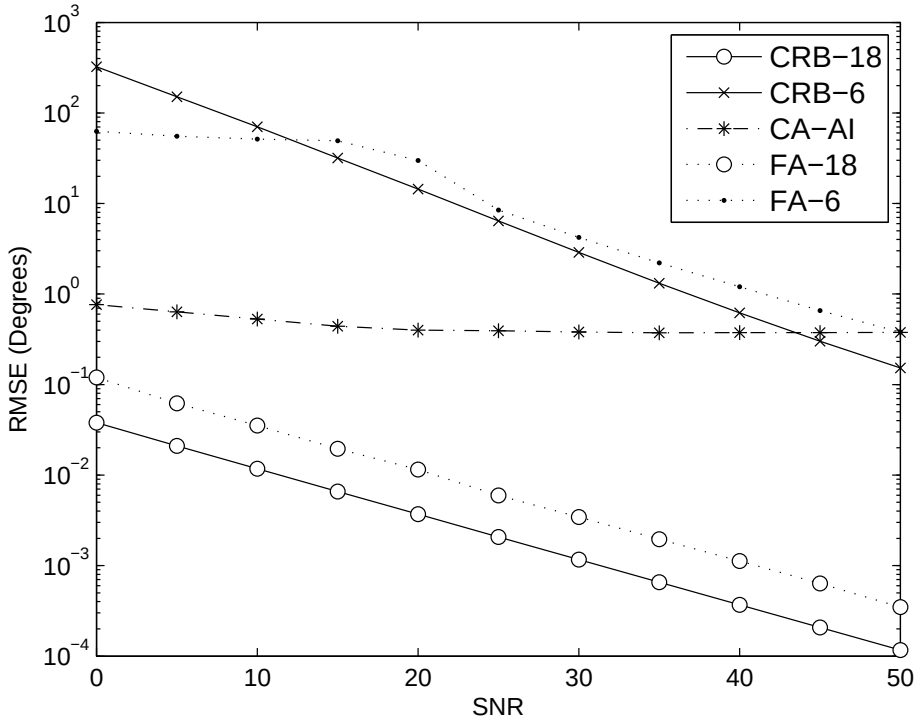

Figure 5.17: Performance for five sources located at 50, 60, 70, 80 and 90 degrees with respect to increasing SNR.

5.1.5 Five Sources

Figures 5.17, 5.18, 5.19 illustrate the hardest problem for a subspace algorithm using an ULA with six sensor elements. Because for five sources in the covariance matrix, noise space $\mathbf{G}$ falls into single dimension. Just by using this single dimension subspace algorithm is forced to find five orthogonal vectors which are also orthogonal to noise space. As seen from Figures 5.17, 5.18, 5.19 interpolated array does a successful estimation compared to six element ULA.

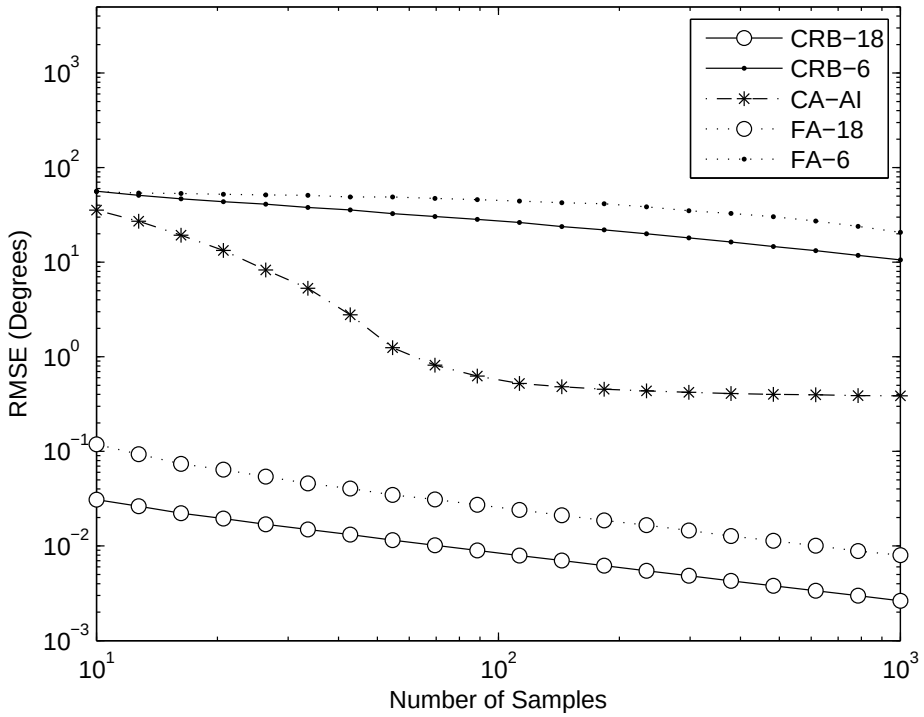

Figure 5.18: Performance for five sources located at 50, 60, 70, 80 and 90 degrees with respect to increasing number of snapshots.

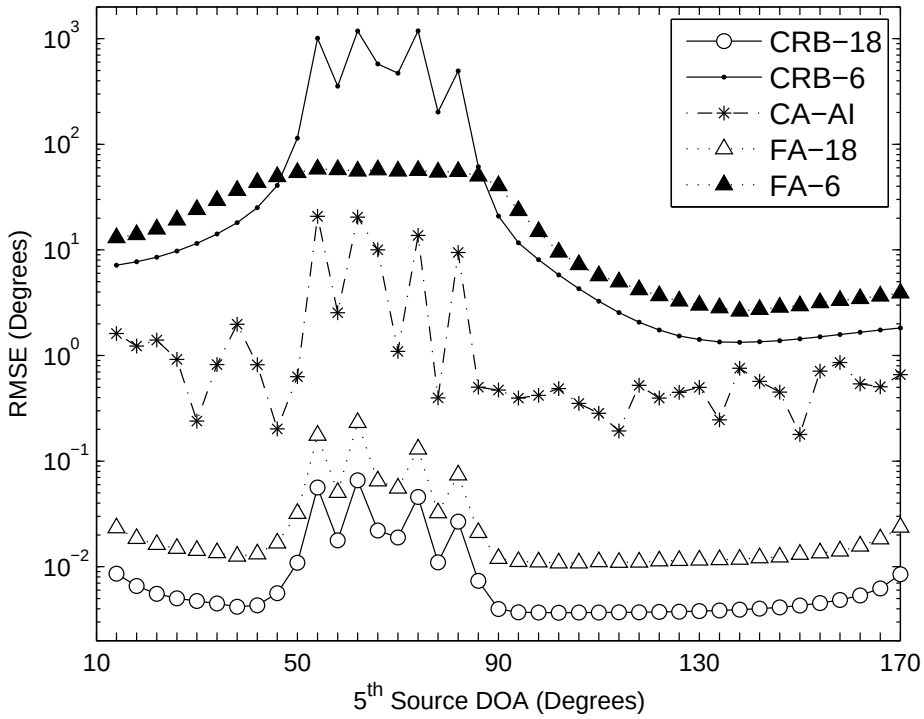

Figure 5.19: Performance for four sources located at 50, 60, 70 and 80 degrees, fifth one is moving 10 to 170 degrees.

5.2 Superior Case

This is the case which the number of sources is equal or greater than the number of sensors in array. For $\tilde{d}_6$ and d_6, six and seven sources cases are investigated further in this section.

5.2.1 Six Sources

In Figure 5.20, graph of ULA that has six elements does not exist because subspace algorithms that use ULA can not locate sensors equal or greater than the sensor elements. This case is called superior case as mentioned before. On the other hand, interpolated NLA allows subspace algorithms to work with superior case. NLA with six sensor elements, does not perform as well as in previous simulations but after the number of snapshots passes the value 100, error is about one degree for six sources.

5.2.2 Seven Sources

In Figure 5.21 six sources fixed at angles 30, 50, 70, 90, 110 and 130 degrees while the seventh source is swept from 10 to 170 degrees. In this experiment two different NLA, which are defined in the beginning of this section as d_6 and $\tilde{d}_6$, are used to illustrate different location of gaps cause different estimation performances because interpolation does not perform identical for different kinds of gap sequences. Note that as long as 7^{th} source is not so close to fixed sources, RMSE appears to be between 1 to 2 degrees.

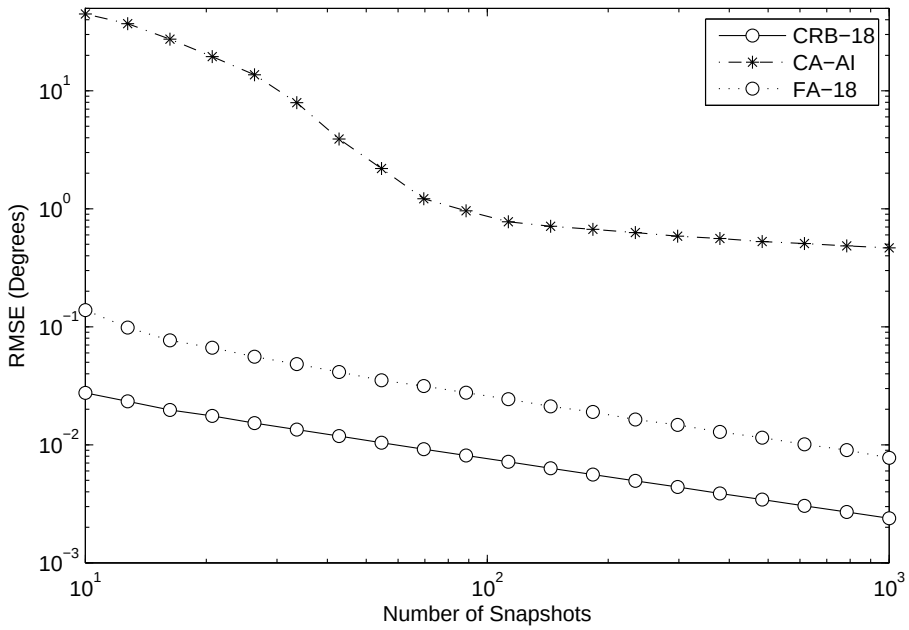

Figure 5.20: Performance for six sources located at 60, 70, 80, 90, 100 and 110 degrees with respect to increasing number of snapshots.

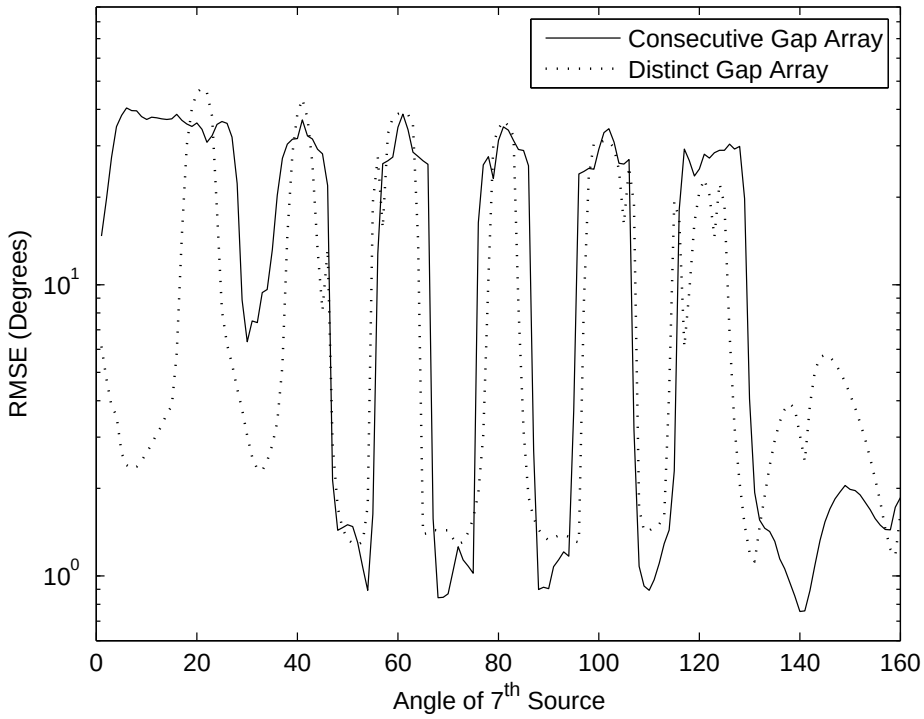

Figure 5.21: Performance for six sources located at 30, 50, 70, 90, 110 and 130 degrees, seventh one is moving 10 to 170 degrees.

CHAPTER 6

CONCLUSION

In this thesis, the improvement of DOA estimation given an initial estimate for nonuniform linear arrays is considered. A new method is proposed which employs array interpolation for NLA. The proposed approach considers a narrow sub-sector for each source and generates a mapping matrix in order to augment the covariance matrix appropriately. A Wiener formulation is derived for the mapping matrix in order to decrease errors during mapping matrix construction.

Advantages and disadvantages of the proposed method are given in the following sections.

6.1 Advantages

As mentioned previously, proposed method basically interpolates a NLA into a ULA. As a result, with a little number of sensors, an array of large aperture size can be obtained with low computational complexity and without angular sector limitations. There are two additional important advantages of a larger array, increased number of source detection capability and better resolution performance.

6.1.1 Number of Sources

As explained in subsection 2.2.2, subspace methods use the covariance matrix of recorded data in sensors. Covariance matrix rank can be at most the number of sensor in a ULA. However, in NLA rank for the covariance matrix of incoming data is more than the number of sensors. Rank of the correlation matrix is equal to all different lags available in the correlation matrix assuming the sources are uncorrelated as defined in subsection 2.1.1. It should be noted that proposed method of interpolation in this discussion does not necessarily increase the rank of covariance matrix, but just fills the gaps in covariance matrix to make it suitable for subspace algorithms.

In section 5.2 Figures 5.20 and 5.21 show that NLA can be used to find six or seven sources which is not even possible for a ULA with six sensors. Therefore proposed method increases the number of sources that can be detected.

6.1.2 Resolution

Resolution is defined as the capability of discriminating two closely spaced sources. This property depends on how wide array aperture is, since biggest time difference of wave arrival on sensor elements occur on the left most and right most positions (endfires). As it is obvious for a fixed number of sensor elements, a NLA has much larger aperture size than a ULA.

Therefore inherently NLA has the advantage of resolving more closely spaced sources than ULA can. This is illustrated in Figures 5.14 and 5.15.

6.1.3 Independency of Angular Sector

Array interpolation methods in literature [47], [42] depends on angular sector. There are two ways to manipulate incoming data, in order to estimate DOA with angular sector dependent algorithms. First, all sources are

assumed to be in a limited angular sector of around 30^0 span, which is an optimistic assumption. Second, if it is possible, all spatial spectrum is divided in 30^0 portions via spatial filtering. Then by using one of these approaches array interpolation performed.

In this thesis, transformation matrix is independent of an angular sector but initial rough estimates of source directions should be given. In a sense, this approach actually uses narrow angular sectors as many as sources. Angular sector independency of the proposed method can be observed in various figures, some of them are Figure 5.6, Figure 5.14.

6.1.4 Low Computational Complexity

Proposed method requires a rough estimation of DOA. This DOA estimates can be obtained by a sub-space method that uses a course estimated correlation matrix. Overhead of total operation for finding $\mathbf{T}$ matrix is composed of finding these initial estimates, that increases the total process time twice.

Alternative approaches [20] for filling the gaps in covariance matrix requires finding initial feasible points and linear programming which requires heavy computational complexity compared to the method proposed in this discussion. Hence, proposed method does not bring any computational complexity at all compared to its alternative.

6.2 Disadvantages

Besides those advantages of a NLA listed in section 6.1 there are some problems such as ambiguity and multi-path phenomena.

6.2.1 Ambiguities

Two non-identical source set may create identical covariance matrix for NLA. This ambiguity results in irrelevant source angle estimations which leads to high mean square estimation errors. This problem is widely investigated in [48], [49], [50], [51]. In this thesis this phenomena is omitted during the calculations.

6.2.2 Multi-Path

Multi-path phenomena as illustrated in Figure 1.1 occurs almost all the time in practical applications. So several studies [24], [45], [25], [52] were conducted to overcome this problem. But unfortunately there is not much study in literature for spatial smoothing in NLA except a method Abramovich presented in [53]. But his solution only valid for small number of correlated sources with specially designed NLA. In this study coherent sources are left outside the discussion. It is the point that is going to be considered in future studies.

REFERENCES

[1] Smith-Rose, R. L., "A sensitive long-wave radio direction-finder," *Journal of Scientific Instruments*, vol.4, no.8, pp.252–262, 1927.

[2] Dolph, C.L., "A Current Distribution for Broadside Arrays Which Optimizes the Relationship Between Beam Width and Side Lobe Levels, " *Proc. I.R.E*, vol.34, pp.335–348, June 1946.

[3] Allen, J. L., "The theory of array antennas (with emphasis on radar applications)," *M.I.T. Lincoln Lab.*, Lexington, Mass., tech. rep. 323, memo DDC AD–422945, July 1963.

[4] Kraus, J. D., "Radio Astronomy. ", McGraw-Hill, New York, 1966.

[5] Yılmaz, Ö., "Akustik Kaynaklar İçin Geliş Açısı Tespiti ve Yönlenme," *Elektrik-Elektronik Mühendisliği Bölümü, Orta Doğu Teknik Üniversitesi*, Kasım 2000.

[6] Wagstaff, R. and Baggeroer, A., editors, "High Resolution Spatial Processing in Underwater Acoustics," *Naval Ocean Research and Development Activity, NSTL* Mississippi 1983.

[7] Haykin S., "Array Signal Processing."Prentice-Hall, Englewood Cliffs, New Jersey, 1985.

[8] Godara, L. C., "Application of antenna arrays to mobile communicaitons. I. Performance improvment, feasibility, and system considirations," *Proceedings of the IEEE* vol.85, no.7, pp.1031–1060, July 1997.

[9] Godara, L. C., "Application of antenna arrays to mobile communications. II. Beam-forming and direction-of-arrival considerations," *Proceedings of the IEEE*, vol.85, no.8, pp.1195–1245, August 1997.

[10] McKeighen, R. E., "Design guidelines for medical ultrasonic arrays," *SPIE International Symposium on Medical Imaging*, vol.3341, pp.218, 1998.

[11] Krim, H. and Viberg, M. "Two decades of array signal processing research, the parametric approach," *IEEE Signal Processing Magazine* vol.13, pp.6794, July 1996.

[12] Rao, B.D. and Hari, K.V.S., "Performance analysis of Root-Music," *Acoustics, Speech, and Signal Processing , IEEE Transactions*, vol.37, no.12, pp.1939–1949, December 1989.

[13] Schmidt, R.O., "A Signal Subspace Approach to Multiple Emitter Location and Spectral Estimation," *Ph.D. Dissertation, Stanford University*, Stanford, CA, November 1981.

[14] Capon J., "High resolution frequency-wavenumber spectrum analysis," *Proceedings IEEE*, vol.57, pp.1408–1418, August 1969.

[15] Paulraj,A., Roy, R. and Kailath, T., "Estimation of signal parameters via rotational invariance techniques - ESPRIT," *In Proc. 19th Asilomar Conf. on Circuits, Systems and Comp.*, pp.83–89, Asilomar, Pacific Grove, CA, November 1985.

[16] A. Kangas, P. Stoica, and T. Soderstrom, "Finite sample and modeling error effects on ESPRIT and MUSIC direction estimators," *Radar, Sonar and Navigation, IEE Proceedings* vol.141, pp.249–255, October 1994.

[17] Ferreol, A., Larzabal, P. and Viberg, M., "On the asymptotic performance analysis of subspace DOA estimation in the presence of modeling errors: case of MUSIC," *Signal Processing, IEEE Transactions*, vol.54, no.3, pp.907–920, March 2006.

[18] Featherstone, W., Strangeways, H.J., Zatman, M.A. and Mewes, H., "A novel method to improve the performance of Capon's minimum variance estimator," *Antennas and Propagation, Tenth International Conference*, vol.1, no.436, pp.322–325, 14–17 April 1997.

[19] Stoica, P., Larsson, E.G. and Gershman, A.B., "The stochastic CRB for array processing: a textbook derivation," *IEEE Signal Processing Letters*,, vol.8, no.5, pp.148–150, May 2001.

[20] Abramovich, Y.I., Spencer, N.K., Gorokhov, A.Y., Detection-estimation of more uncorrelated Gaussian sources than sensors in nonuniform linear antenna arrays. II. Partially augmentable arrays, IEEE Trans. on Signal Proc., , vol.51, no.6, pp.1492–1507, June 2003.

[21] Abramovich, Y.I., Spencer, N.K. and Gorokhov, A.Y., "Positive-definite Toeplitz completion in DOA estimation for nonuniform linear antenna arrays. II. Partially augmentable arrays," *IEEE Trans. on Signal Proc.*, vol.47, no.6, pp.1502–1521, June 1999.

[22] Pillai, S. and Haber, F., "Statistical analysis of a high resolution spatial spectrum estimator utilizing an augmented covariance matrix," *IEEE Trans. on Signal Processing*, vol.35, no.11, pp.1517–1523, November 1987.

[23] Kumaresan, R. and Tufts, D. W., "Estimating the angles of arrival of multiple plane waves," *IEEE Trans. Aerosp. Electron. Syst.*, vol.AES-19, pp.134–139, January 1983.

[24] Tie-Jun Shan, Wax, M. and Kailath, T. "On spatial smoothing for direction-of-arrival estimation of coherent signals," *Acoustics, Speech, and Signal Processing [see also IEEE Transactions on Signal Processing], IEEE Transactions*, vol.33, no.4, pp.806–811, August 1985.

[25] Li, J., "Improved angular resolution for spatial smoothing techniques," *Signal Processing, IEEE Transactions on [see also Acoustics, Speech, and Signal Processing, IEEE Transactions on]*, vol.40, no.12, pp.3078–3081, December 1992

[26] Choi, Y.-H., "Subspace-based coherent source localisation with forward/backward covariance matrices," *Radar, Sonar and Navigation, IEE Proceedings*, vol.149, no.3, pp.145–151, June 2002.

[27] Zaghloul, A. and MacPhie, R. "On the removal of blindness in phased antenna arrays by element positioning errors," *Antennas and Propagation, IEEE Transactions on [legacy, pre - 1988]*, vol.20, no.5, pp.637–641, September 1972.

[28] Flanagan, B.P., Bell, K.L. "Improved array self calibration with large sensor position errors for closely spaced sources," *Sensor Array and Multichannel Signal Processing Workshop. 2000.*, Proceedings of the 2000 IEEE, pp.484–488, 2000.

[29] Stoica, P. and Moses R., "Introduction to Spectral Analysis"Englewood Cliffs, NJ: Prentice-Hall, 1997.

[30] Trees, H.V., "Optimum array processing." John Wiley, New York. USA, 2002.

[31] Weiss, A.J. and Friedlander, B., "On the Cramer-Rao Bound for Direction Finding of Correlated Signals," *Signal Processing, IEEE Transac-*

tions on [see also Acoustics, Speech, and Signal Processing, IEEE Transactions on] vol.41, no.1, pp.495–, Jan 1993.

[32] Scharf, L.L. and McWhorter, L.T., "Geometry of the Cramer-Rao bound," *Statistical Signal and Array Processing, 1992. Conference Proceedings., IEEE Sixth SP Workshop on*, pp.5–8, 7–9 October 1992

[33] Stoica, P. and Nehorai Arye, "MUSIC, maximum likelihood, and Cramer-Rao bound," *Acoustics, Speech, and Signal Processing [see also IEEE Transactions on Signal Processing], IEEE Transactions on*, vol.37, no.5, pp.720–741, May 1989.

[34] Stoica, P., Nehorai, A., "MUSIC, maximum likelihood, and Cramer-Rao bound: further results and comparisons," *Acoustics, Speech, and Signal Processing [see also IEEE Transactions on Signal Processing], IEEE Transactions on*, vol.38, no.12, pp.2140–2150, December 1990.

[35] Stoica, P., Jian Li, "Study of the Cramer-Rao bound as the numbers of observations and unknown parameters increase," *Signal Processing Letters, IEEE* vol.3, no.11, pp.299–300, November 1996.

[36] Gershman, A.B., Stoica, P., Pesavento, M. and Larsson, E.G., "Stochastic Cramer-Rao bound for direction estimation in unknown noise fields," *Radar, Sonar and Navigation, IEE Proceedings*, vol.149, no.1, pp.2–8, February 2002.

[37] Stoica, P. and Moses R., "Spectral Analysis of Signals." Prentice-Hall, Upper Saddle River, NJ, 2005.

[38] Haubrich, R.A., "Array design," *Bull. Seismol. Soc. Am.*, vol.58, no.3, pp.977–991, June 1968.

[39] Leech, J., "On the representation of 1, 2. . . . , 71 by differences," *J.London Math. Soc.*, vol.31, pp.160–169, 1956.

[40] Sverdlik, M.B., "Optimal discrete signals," *Moscow, Sovetskoe Radio*, pp.200, 1975.

[41] Bronez, T.P., "Sector interpolation of non-uniform arrays for efficient high resolution bearing estimation," *International Conference on Acoustics, Speech, and Signal Processing, ICASSP-88*, vol.5, pp.2885–2888, April 1988.

[42] Hyberg, P., Jansson, M. and Ottersten, B., "Array Interpolation and DOA MSE Reduction," *IEEE Trans. on Signal Processing*, vol.53, no.12, pp.4464–4471, December 2005.

[43] Friedlander, B. and Weiss, A.J., "Direction finding for wide-band signals using an interpolated array," *IEEE Trans. on Signal Processing*, vol.41, no.5, pp.1881–1892, May 1993.

[44] Hyberg, P., Jansson, M. and Ottersten, B. "Array interpolation and bias reduction," *IEEE Trans. on Signal Proc.*, vol.52, no.10, part 1, pp.2711–2720, October 2004.

[45] Friedlander, B. and Weiss, A.J., "Direction finding using spatial smoothing with interpolated arrays," *IEEE Trans. on Aerospace and Electronic Systems*, vol.28, no.2, pp.574-587, April 1992.

[46] Indukumar, K.C., Reddy, V.U., "A note on redundancy averaging," *IEEE Trans. on Signal Proc.*, vol.40, no.2, pp.466 – 469, February 1992.

[47] Friedlander, B., "Direction finding using an interpolated array," *Acoustics, Speech, and Signal Processing, 1990. ICASSP-90., 1990 International Conference on* pp.2951–2954, vol.5, 3–6 April 1990.

[48] Abramovich, Y.I., Spencer, N.K. and Gorokhov, A.Y., "Resolving manifold ambiguities in direction-of-arrival estimation for nonuniform linear

antenna arrays," *IEEE Trans. Signal Processing*, vol.47, pp.2629-2643, October 1999.

[49] Proukakis C. and Manikas A., "Study of ambiguities of linear arrays," *in Proc. ICASSP* vol.4, pp.549552, Adelaide, Australia, 1994.

[50] Manikas A. and Proukakis C., "Modeling and estimation of ambiguities in linear arrays," *IEEE Trans. Signal Processing*, vol.46, pp.2166-2179, August 1998.

[51] Abramovich, Y.I., Gaitsgory V.G. and Spencer, N.K., "Stability of manifold ambiguity resolution in DOA estimation with nonuniform antenna arrays," *AEU Int. J. Electron. Commun.* vol.53, no.6, pp.364-370, 1999.

[52] Williams, R.T., Prasad, S., Mahalanabis, A.K. and Sibul, L.H., "An improved spatial smoothing technique for bearing estimation in a multipath environment," *Acoustics, Speech, and Signal Processing , IEEE Transactions on*, vol.36, no.4, pp.425–432, April 1988.

[53] Abramovich, Y.I. and Spencer, N.K., "Simultaneous DOA estimation of fully correlated and uncorrelated Gaussian sources in nonuniform linear antenna arrays," *Proceedings of the 8th Annual Workshop on Adaptive Sensor Array Processing (ASAP 2000)*, pp 73–78, MIT Laboratory, Lexington, Massachusetts, USA, March 2000.